Kinetics of Reaction of Nitrite with Deoxy Hemoglobin after Rapid Deoxygenation or Predeoxygenation by Dithionite Measured in Solution and Bound to the Cytoplasmic Domain of Band 3...

ARTICLE *in* BIOCHEMISTRY · JULY 2008

Impact Factor: 3.02 · DOI: 10.1021/bi8000819 · Source: PubMed

1 AUTHOR:

James M Salhany
The Nebraska Medical Center
103 PUBLICATIONS **1,734** CITATIONS

SEE PROFILE

Kinetics of Reaction of Nitrite with Deoxy Hemoglobin after Rapid Deoxygenation or Predeoxygenation by Dithionite Measured in Solution and Bound to the Cytoplasmic Domain of Band 3 (SLC4A1)‡

James M. Salhany*

Departments of Internal Medicine and Biochemistry and Molecular Biology, University of Nebraska Medical Center, 984510 Nebraska Medical Center, Omaha, Nebraska 68198-4510

Received January 15, 2008; Revised Manuscript Received March 17, 2008

ABSTRACT: The reaction of deoxyhemoglobin with nitrite was characterized in the presence of dithionite using hemoglobin in solution or bound to the cytoplasmic domain of band 3 (CDB3). Deoxyhemoglobin was generated by predeoxygenation (nitrogen flushing followed by addition of dithionite), or transiently, by rapidly mixing oxyhemoglobin with nitrite and dithionite simultaneously. Wavelength-dependent kinetic studies confirmed the formation of nitrosyl hemoglobin. Furthermore, the rate of reaction was independent of dithionite concentration, indicating that dithionite does not reduce nitrite to nitric oxide directly. Model simulation studies showed that superoxide anion generated by dithionite reduction of molecular oxygen was not a factor in the reaction kinetics. CDB3-bound hemoglobin reacted faster with nitrite than did hemoglobin in solution. This difference was most pronounced for predeoxygenated hemoglobin and least pronounced for rapidly deoxygenated hemoglobin. The smaller difference observed in the rapid deoxygenation experiment was associated with much faster kinetics compared to the predeoxygenation experiment. Model simulation studies showed, and literature evidence indicates, that faster kinetics in the rapid deoxygenation experiment were related to the initial presence of R-state Hb(II)O_2 $\alpha\beta$ dimers, both in dilute solution and when bound to CDB3. Thus, rapidly deoxygenated CDB3-bound hemoglobin $\alpha\beta$ dimers react 5-fold faster with nitrite than predeoxygenated tetrameric hemoglobin in solution. Faster nitrite reductase kinetics for CDB3-bound hemoglobin suggests the possibility of preferential nitric oxide generation at the inner surface of the erythrocyte membrane, thus coupling the release of oxygen from hemoglobin to the production and successful release of nitric oxide from the erythrocyte, and the regulation of blood flow.

The reaction of NO[1] with Hb(II) has been studied for over three decades (*1*). Interest in the properties of Hb(II)NO accelerated in the 1970s when it was discovered that it could be switched from the high affinity R- to the low affinity T-quaternary conformational state without dissociation of NO. Switching occurred when the allosteric effector molecule IHP was added to Hb(II)NO (*2–7*). Switching could also be induced even in the absence of allosteric effectors, by simply replacing CO with NO at the hemes of hemoglobin Kansas (α_2 $\beta_2$102 Asn → Thr) (*5*). These findings offered general support for the two-state allosteric model of Monod, Wyman, and Changeux (*8*).

Today, NO has become physiologically relevant, in light of discoveries showing that it is produced from endothelial NO synthase and participates in the regulation of basal blood vessel tone and vascular homeostasis (*9–13*). The involvement of the erythrocyte in regulation of microvascular tone was first suggested by experiments showing that the oxygen-linked R-state to T-state transition within the hemoglobin tetramer (*8*) was associated with ATP release from the cell, with ATP binding to purinergic receptors in the endothelium resulting in vasodilatation (*14, 15*). An alternate hypothesis suggested that hemoglobin deoxygenation resulted in NO release from the erythrocyte and that such release caused subsequent NO-dependent vasodilatation (*16–19*).

Two fundamentally different mechanisms have been proposed to explain the oxygen-linked release of NO from the red cell. One mechanism suggests that NO reacts with the β-93 −SH group of Hb(II)O_2 to form S-nitroso hemoglobin (*16*). It is known that the β-93 −SH group is more reactive in the oxygenated R-state than in the deoxy T-state (*1*). This difference could potentially serve to link NO binding and release to oxygen binding to Hb(II), and therefore to oxygen demand and blood flow. Alternatively, it has been proposed that plasma NO_2^- can be converted

‡ This article is dedicated to the memory of Dr. Robert Cassoly.

* To whom correspondence should be addressed. Phone: 402-559-6281. E-mail: jsalhan@attglobal.net.

[1] Abbreviations: NO, nitric oxide; NO_2^-, nitrite; NO_2, nitrogen dioxide; N_2O_3, nitrous anhydride (dinitrogen trioxide); $ONOO^-$, peroxynitrite; NO_3^-, nitrate; ONOOH, peroxynitrous acid; N_2O, nitrous oxide; SO_2^-, dithionite monomer; $S_2O_4^{-2}$, dithionite dimer; O_2^-, superoxide anion; H_2O_2, hydrogen peroxide; P_i, orthophosphate, P_iNO, P_i and NO binary complex; RSH, organic thiol group; RSNO, NO-bound organic thiol; Hb(II)NO, nitrosyl hemoglobin; Hb(III), ferric hemoglobin; Hb(II), deoxygenated ferrous hemoglobin; Hb(II)O_2, oxyhemoglobin; ATP, adenosine triphosphate; IHP, inositol hexaphosphate; 2,3-DPG, 2,3-diphosphoglycerate; CDB3, cytoplasmic domain of band 3.

10.1021/bi8000819 CCC: $40.75
Published on Web 05/09/2008

into NO by the NO_2^- reductase activity of intracellular deoxy Hb(II) (*17–19*).

One major challenge facing hypotheses suggesting that NO is released from red cells during deoxygenation is that the affinity of deoxy Hb(II) for NO is high ($K_d \approx 10^{-12}$ to 10^{-13} M). This value was derived from the large value of the rate constant for the reaction of NO with Hb(II) (2.4×10^7 M^{-1} s^{-1}) (*20*), and the small value of the rate constants for NO release from the T-state (1×10^{-3} s^{-1}) and from the R-state (9.5×10^{-6} s^{-1}) (*7*). A small K_d value, in combination with a high concentration of intracellular hemoglobin (~20 mM on a heme basis), suggests that NO generated by the NO_2^- reductase reaction or released from β-93 −SH groups should never escape from the deoxygenating erythrocyte, yet it clearly does (*21*). A possible solution to this problem would be if NO_2^- reacted preferentially with membrane-bound hemoglobin. This would allow for the formation of NO at the inner surface of the membrane, where the probability for successful release from the cell might be higher than that from hemoglobin within the cytosolic space.

Both Hb(II) and Hb(II)O_2 have been shown to bind to the cytoplasmic domain of band 3 (CDB3) (*22–32*), the erythrocyte trans-membrane anion exchange protein. Hb(II)O_2 has been shown to bind predominantly as $\alpha\beta$ dimers (*23, 24, 27, 28*), while Hb(II) binds as the tetramer (*23, 25, 26, 28–30*). There is disagreement as to which species binds the tightest, Hb(II)O_2 $\alpha\beta$ dimers (*25, 26*), or deoxy Hb(II) tetramers (*29, 30*). Furthermore, it has not been established whether Hb(II) and Hb(II)O_2 bind to the same site on CDB3. X-ray crystallographic evidence showed that the acidic N-terminal peptide of CDB3 binds to the central cavity of Hb(II) where 2,3-DPG binds (*29*). Oxygenation of Hb(II) would be expected to cause a change in the quaternary conformational state, which should make the CDB3 binding site inaccessible. However, dissociation of Hb(II)O_2 tetramers to $\alpha\beta$ dimers should expose at least part of the CDB3 binding site on one hemoglobin $\alpha\beta$ dimer, thus favoring preferential binding of Hb(II)O_2 $\alpha\beta$ dimers versus Hb(II)O_2 tetramers. Finally, although one might initially suggest that there are no Hb(II)O_2 dimers present at the high concentration of intracellular hemoglobin present in the red cell, calculations have shown that the concentration of dimers may be as high as 100 μM, assuming a 3 μM Hb(II)O_2 tetramer to dimer dissociation constant at physiological pH and ionic strength (*23*). This would be enough to saturate band 3 sites, assuming that Hb(II)O_2 $\alpha\beta$ dimers have a sufficiently high affinity for CDB3 sites (*25, 26, 31, 32*).

I have performed a series of experiments involving the use of dithionite to study the NO_2^- reductase reaction of hemoglobin in solution and bound to CDB3. This protocol compares the reaction of NO_2^- with Hb(II) generated by rapid deoxygenation of R-state Hb(II)O_2, to the reaction of NO_2^- with predeoxygenated T-state Hb(II) tetramers. These reactions were performed using hemoglobin in dilute solution and bound to CDB3. I also characterize the role of dithionite in this reaction for the first time. This experimental work was supplemented by detailed model simulation studies that focused on the role: (a) of side reactions involving O_2^-, NO, dithionite, and hemoglobin in the overall kinetic behavior of the system and (b) of hemoglobin dimer−tetramer association−dissociation kinetics in the reaction of NO_2^- with deoxy Hb(II) generated during the rapid deoxygenation experiment.

MATERIALS AND METHODS

Fresh in-dated erythrocytes were obtained from the Omaha Chapter of the American Red Cross. ACS reagent grade sodium nitrite was obtained from Sigma and purified grade sodium dithionite from Fisher Scientific. All other chemicals were reagent grade.

Erythrocytes were washed and hemolysates prepared as described (*33*). After centrifugation to remove membranes, Hb(II)O_2 hemolysates were dialyzed extensively in 5 mM sodium phosphate, pH 8.0 (5P(8)) buffer at 4 °C. Samples were then dialyzed in the same buffer at various pH values. Optical spectra were measured in a Genesys 2 spectrometer (Thermo Fisher Scientific). Hemoglobin-free, salt stripped unsealed ghosts were prepared as described (*24*).

Rapid deoxygenation experiments were performed by simultaneously mixing Hb(II)O_2 with NO_2^- and dithionite under the specific experimental conditions described below. Predeoxygenated Hb(II) was prepared by flushing with nitrogen to remove molecular O_2 and then adding crystals of sodium dithionite under positive nitrogen flow. Sample pH was measured under positive nitrogen flow after addition of dithionite and the pH adjusted if necessary. These samples were transferred to the stopped-flow apparatus anaerobically. Static optical spectra for predeoxygenated Hb(II) were measured in cuvettes capped with rubber stoppers, which were flushed with nitrogen, and into which the Hb(II)/dithionite solutions were injected with a syringe.

Stopped-flow experiments were performed using a single beam Gibson−Durrum stopped-flow apparatus. The apparatus has been described in detail in a review by Gibson (*34*). Collection of primary data from the stopped-flow was performed essentially as described in reports from this laboratory (*35*). In brief, 1000 data points were collected per stopped-flow mix, with a given time course consisting of an average of at least three to 10 such mixes per condition, with the number depending on the signal-to-noise level. The data were saved and imported into Sigma Plot (SPSS Science, Chicago IL) for further analysis. Initial velocities were calculated by fitting data within the linear initial 30% of each time course (see below) using the linear least-squares analysis available in Sigma Plot. The slope so determined was then multiplied by the concentration of hemoglobin present in the samples initially after the mix (see legend to Figure 4). That value then was plotted against its respective concentration of NO_2^-. Model simulation studies were performed using Chemical Kinetics, version 1.01, provided online by the IBM Almaden Research Center (*36*). Analysis of the experimental and simulated data and graphic presentations of the results were performed using Sigma Plot. Determination of p*K* values was performed using Enzfitter (*37, 38*).

RESULTS

Experimental Studies. Reaction of NO_2^- with Predeoxygenated Hb(II) in Solution in the Presence of Dithionite. The use of dithionite to rapidly deoxygenate hemoglobin has been studied extensively under various conditions (*39–44*). Release of O_2 from Hb(II)O_2 in solution is promoted by rapid

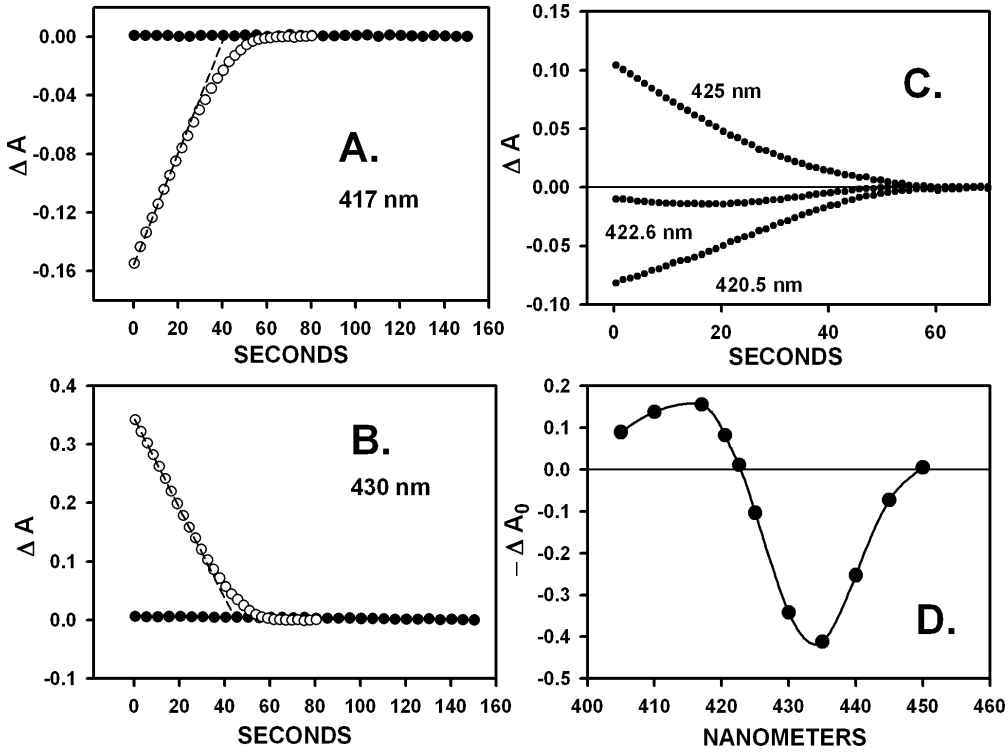

FIGURE 1: Spectral-kinetic studies of the reaction of predeoxygenated Hb(II) with NO_2^- in the presence of dithionite in solution. Hb(II) (12.6 μM, before mixing in the stopped-flow apparatus) was prepared as described in Materials and Methods. The final dithionite concentration was 10 mM, and a final measured pH was 6.75. This sample was anaerobically transferred to the Gibson-Durrum stopped-flow apparatus. Five millimolar sodium phosphate buffer containing (○) or lacking (●) 20 mM sodium nitrite was flushed with nitrogen, and crystals of sodium dithionite were added to yield a final concentration of 10 mM, pH 6.75. These latter samples were mixed 50:50 in the Gibson-Durrum stopped-flow apparatus at 25 °C, with the Hb(II) solution. (A) Reaction time course at 417 nm. (B) Reaction time course at 430 nm. The symbols have the same meaning as in A. (C) Wavelength dependence near a Soret isosbestic point. There was no well-defined kinetic isosbestic point, indicating the presence of a third species. (D) Plot of the amplitude ($-\Delta A_0$) of reactions like those in panels A−C versus wavelength. The dashed lines in panels A and B were drawn by eye.

scavenging of unbound O_2 by dithionite. Dithionite first reduces all of the unbound O_2 to O_2^- in a rapid reaction (*45, 46*) and then reacts with the O_2 that is more slowly released from Hb(II)O_2. The rate of this latter reaction is essentially independent of the concentration of dithionite (*40, 41*).

A novel and potentially important use for dithionite in the field of NO transport by the human erythrocyte was indicated in the brief description given on page 42 of the book on hemoglobin by Antonini and Brunori (*1*). They stated that when NO_2^- was added to a Hb(II) solution containing dithionite, Hb(II)NO was generated. Apparently this phenomenon was not studied further. In the present study, dithionite is used to ensure oxygen-free conditions and to reduce Hb(III) generated by the reductase reaction back to Hb(II). Thus, it seemed important to both experimentally substantiate that Hb(II)NO is formed under the stated conditions and to experimentally and theoretically establish the overall mechanism.

There are three possible mechanisms to explain the Antonini−Brunori Effect: (a) direct (noncatalytic) reaction of NO_2^- with dithionite to produce NO,

$$S_2O_4^{-2} + 2NO_2^- \rightarrow 2SO_3^{-2} + 2NO \quad k_1 \qquad (1)$$

and subsequent reaction of NO with Hb(II), (b) reaction of NO_2^- with dithionite in the presence of an iron catalyst (*47*), (possibly Hb(II)) to produce NO, which subsequently reacts with Hb(II), and (c) the direct reaction of Hb(II) with NO_2^- to produce NO, independent of dithionite concentration. In this latter mechanism, dithionite simply functions to remove O_2 from the system. With regard to possibility (a), experimental work by Makarov and co-workers (*48*) has shown that there was no significant direct reaction between dithionite and NO_2^- in solution between 15° and 50 °C. Thus, I have studied the kinetics of reaction of NO_2^- with Hb(II) in the presence of dithionite to discriminate between possibilities (b) and (c).

The spectral-kinetic results for the reaction of NO_2^- with predeoxygenated Hb(II) are shown in Figure 1 (A−D). Figure 1A and B shows that the absorbance increase at 417 nm and decrease at 430 nm are linear for about the first 30% to 50% of the time course. Figure 1C illustrates the wavelength dependence of the time course near the 423 nm static isosbestic point (*7*). No wavelength could be found in this region that gave an absolute kinetic isosbestic point, where no change in absorbance was observed over the course of the reaction. This indicates the presence of a third spectral-kinetic species. This conclusion is supported by the 422.6 nm time course, which is biphasic. Figure 1D shows the wavelength dependence of the total absorbance change for the reaction of NO_2^- with predeoxygenated Hb(II) in the presence of dithionite. This difference spectrum is the inverse of the one generated by Moore and Gibson (*7*) for the conversion of Hb(II)NO to Hb(II) and indicates that the reactions in Figure 1 represent the loss of Hb(II) and the formation of Hb(II)NO. Therefore, when NO_2^- is mixed with Hb(II) in the presence of dithionite, Hb(II)NO is formed (*1*).

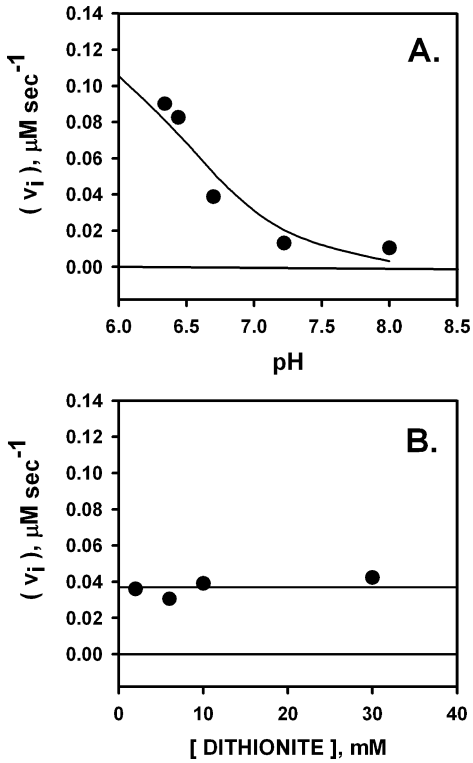

FIGURE 2: pH and dithionite dependence of the reaction of predeoxygenated Hb(II) with NO_2^- in solution. (A) pH dependence of the initial velocity (v_i) for the disappearance of Hb(II) at constant dithionite. The reactions were performed as described for the experiments in Figure 1, at 430 nm and 25 °C. The NO_2^- concentration was 5 mM, with dithionite concentration fixed at 10 mM, both after the mix. pH values were determined after mixing under positive nitrogen flow as described in Materials and Methods. The apparent p*K* was determined using the Enzfitter program containing the equation: $v_i = [(v_1) + \{(v_2) * 10^{(pH - pK)}\}]/[1 + 10^{(pH - pK)}]$, where v_1 and v_2 are the values of the initial velocities at the upper and lower limits of the titration curve, respectively. The value of v_1 was 0.15 ± 0.03 μM s^{-1}, and the value of v_2 was 0.001 ± 0.01 μM s^{-1} with an apparent p*K* of 6.45 ± 0.23. (B) Dithionite concentration dependence of v_i at constant pH. This reaction was measured at 430 nm, 25 °C, and at constant NO_2^- concentration (5 mM after mixing) at pH 6.71. The concentration of Hb(II) was 6.6 μM after mixing.

Figure 2A and B shows the pH and dithionite dependences, respectively, for the reaction of predeoxygenated hemoglobin with NO_2^-. The apparent reaction p*K* was estimated to be 6.45 ± 0.23. This is essentially the same as the pH dependence for the reaction of NO_2^- with dithionite, catalyzed by an organic metal−ion complex (*47*). That suggests that NO may be formed from NO_2^- and dithionite through the iron catalysis mechanism (*47*). However, there was no dependence of the reaction on dithionite concentration (Figure 2B). For the catalyzed reaction involving the organic metal−ion complex (*48*), the rate increased 4-fold with increasing dithionite concentration. The concentration range used here is ~4-fold larger than the dithionite concentration range used in that study, yet there was no significant change in rate. Thus, prereaction of NO_2^- with dithionite in the presence of an organo-metalic catalyst is not part of the mechanism involved in the formation of Hb(II)NO.

Feasibility Study and Wavelength Dependence for the Reaction of NO_2^- with Hb(II) Generated by Rapid Deoxygenation of Hb(II)O_2 in the Presence of Dithionite. Though predeoxygenation of hemoglobin solutions is a viable means

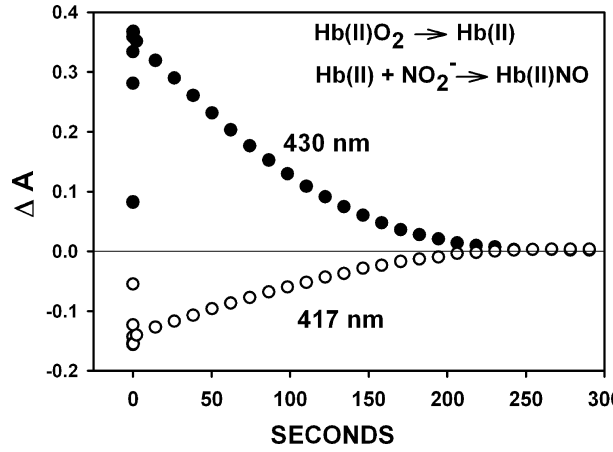

FIGURE 3: Wavelength dependence for the reaction in solution, where Hb(II)O_2 is mixed with dithionite and NO_2^- simultaneously. Hb(II)O_2 (11 μM) in 5 mM sodium phosphate buffer at pH 6.45 was mixed 50:50 in the stopped-flow apparatus with 10 mM sodium dithionite and 1 mM $NaNO_2^-$ in the same buffer at 25 °C. The reaction was studied as a function of wavelength. In this reaction, there is an initial, very rapid, and wavelength dependent absorbance change associated with deoxygenation of Hb(II)O_2, followed by the slower reaction with NO_2^-.

for studying the reaction of NO_2^- with Hb(II), an alternative approach is to study the reaction of NO_2^- with Hb(II) generated by rapid deoxygenation. A rapid deoxygenation experiment may be relevant to the dynamics associated with deoxygenation of hemoglobin when the oxygenated erythrocyte enters the capillary bed.

The overall feasibility of the rapid deoxygenation experiment is illustrated in Figure 3, which shows an experiment at pH 6.45 and 0.5 mM sodium nitrite, where Hb(II)O_2 in solution at ambient pO_2 is mixed with a solution containing NO_2^- and dithionite. At 430 nm (the Soret absorbance peak for Hb(II) (*1*)), there is an initial, very rapid increase in absorbance. After this initial burst phase, there is a slower loss of absorbance at 430 nm. The burst phase has kinetics consistent with the deoxygenation of Hb(II)O_2. I have confirmed my earlier measurements (*41*) showing that the rapid deoxygenation reaction has an apparent rate constant of 59 s^{-1}, at 25 °C, pH 6.5, independent of dithionite concentration (data not shown). Thus, Hb(II)O_2 deoxygenation is complete in about 50 ms. When the measurements were made at 417 nm, the sign and amplitude of both phases change. The amplitude of $\Delta\epsilon_{max}$ for the reaction at 430 nm for rapid deoxygenation, differed from the amplitude of $\Delta\epsilon_{max}$ for the reaction at 430 nm for predeoxygenated Hb(II) (Figure 1B) by ≤10%. This is consistent with rapid formation of Hb(II) in the rapid deoxygenation experiment. The results just presented indicate that it is feasible to study the reactions of Hb(II) with NO_2^- by mixing a solution of Hb(II)O_2 in the stopped-flow apparatus with solutions of NO_2^- and dithionite.

NO_2^- Concentration Dependence of the Reaction of Predeoxygenated and Rapidly Deoxygenated Hb(II), Measured Using Hemoglobin in Solution or Bound to CDB3 at the Inner Surface of Isolated Human Erythrocyte Membranes.

In order to test for differences in the reactivity between rapidly deoxygenated and predeoxygenated Hb(II), the NO_2^- concentration dependence of the reductase reaction was measured. The starting material was: (a) predeoxygenated Hb(II) in solution, (b) predeoxygenated Hb(II) bound to

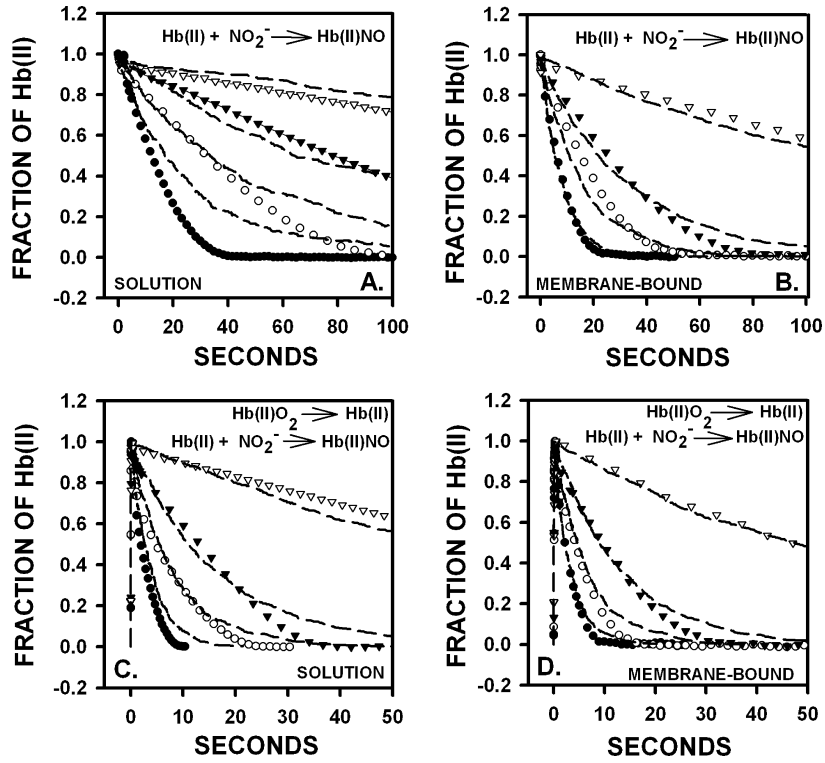

FIGURE 4: Experimental (symbols) and simulated (dashed curves) time courses for the reaction with NO_2^- of predeoxygenated [Hb(II) + NO_2^- → Hb(II)NO] or rapidly deoxygenated [Hb(II)O_2 → Hb(II) and then Hb(II) + NO_2^- → Hb(II)NO] hemoglobin. The fraction of Hb(II) present is defined as ($\Delta A/\Delta A_{max}$) at 430 nm for the experimental time courses and as ([Hb(II)]/[Hb(II)]$_{max}$) for the time courses from the model simulation studies. Furthermore, ΔA_{max} and [Hb(II)]$_{max}$ are defined as the maximum values reached in each case, after rapid deoxygenation of Hb(II)O_2 by dithionite. For predeoxygenatated Hb(II), those values are defined as the initial (time = 0) values. The reactions were measured at various concentrations of nitrite, using hemoglobin in solution (A and C) or bound to the cytoplasmic domain of band 3 (CDB3) on isolated human erythrocyte membranes (B and D). The experimental NO_2^- concentrations after mixing in the stopped-flow apparatus were the same for each deoxygenation condition: (▽) = 0.5 mM; (▼) = 2.5 mM, (○) = 5 mM, and (●) = 10 mM. These reactions were performed as described in the legend to Figure 1, at 430 nm and 25 °C, but with the concentration of dithionite set at 5 mM after mixing. The experimental pH values were 6.5 ± 0.1. The concentration of hemoglobin after the mix was 6.3 μM in the predeoxygenation experiments, and 5.5 μM for the rapid deoxygenation experiment. The simulations presented in this figure were generated as described in the Results section of the text. The initial concentrations of species for the rapid deoxygenation simulation were as follows: [Hb(II)O_2] = 5.5 μM; [Pi] = 5 mM; [$S_2O_4^{-2}$] = 5 mM; [SO_2^-] = 2.6 μM; [O_2] = 270 μM; [H^+] = 3.16 × 10^{-7} M (for pH 6.5); [RSH-per heme] = 2.75 μM; [Hb(III)] = [Hb(III)NO] = [Hb(III)(NO_2^-)] = [deoxy Hb(II)] = [NO] = [Hb(II)NO] = [SO_2] = [O_2^-] = [N_2O_3] = [PiNO] = [RSNO] = [$ONOO^-$] = [HONOO] = [NO_3^-] = [NO_2] = [H_2O_2] = [Hb(II)(NO_2^-)] = 0. The initial concentrations used for the predeoxygenated Hb(II) simulation were the same as that given for the rapid deoxygenation experiment, with the following exceptions: [deoxy Hb(II)] = 6.3 μM; [Hb(II)O_2] = 0 μM; [RSH- per heme] = 0 μM; [O_2] = 0 μM. The values for the rate constants used in a given panel for the reductase part of the mechanism (see the text) are given in Table 1. The other rate constants were taken from Tables 2−4. (A) Reaction of predeoxygenated hemoglobin with NO_2^- in solution. (B) Reaction of predeoxygenated hemoglobin bound to CDB3, with various concentrations of NO_2^- under the same conditions as in panel A. Greater than 98% of the Hb(II) was bound to the membrane, as determined by centrifugation of the sample, and measurement of the absorbance spectrum of the supernate, as well as by visual inspection of the centrifuged membrane pellet. (C) Reaction of Hb(II) in solution generated by rapid deoxygenation of Hb(II)O_2 by mixing with dithionite and NO_2^- simultaneously. Note that in this reaction, there is a very rapid increase in absorbance at 430 nm, due to deoxygenation of Hb(II)O_2. This change is followed by a slower decrease in absorbance as deoxygenated Hb(II) reacts with NO_2^- to form Hb(II)NO. (D) Reaction with NO_2^-, of membrane-bound Hb(II) generated by rapid deoxygenation of Hb(II)O_2 as described for panel C. Visual and spectroscopic confirmation of >98% Hb(II)O_2 bound to the membrane, performed in a manner similar to that described in panel B for deoxy Hb(II).

CDB3 on isolated human erythrocyte membranes (*23*), (c) Hb(II)O_2 in dilute solution (rapid deoxygenation), and (d) Hb(II)O_2 bound to CDB3 on isolated human erythrocyte membranes (*23*) (rapid deoxygenation). All of the measurements were made at 25 °C, at pH 6.5 ± 0.1, as described in the legend to Figure 4. These conditions are those necessary for maximum binding of hemoglobin to band 3 (*23, 24, 28, 31*). It is important to note that both Hb(II)O_2 and Hb(II) were >98% bound to the membrane. This was established by measuring the absorbance of the supernatant fraction in the Soret region of the hemoglobin spectrum, after centrifugation of the membrane suspension as described previously (*31*). This method and visual inspection of the supernate and the membrane pellet were also applied to samples after the reaction, by collecting material expelled from the stopped-flow apparatus.

Figure 4 shows time courses for NO_2^- reacting with predeoxygenated Hb(II) in dilute solution (Figure 4A); predeoxygenated Hb(II) bound to CDB3 (Figure 4B); rapidly deoxygenated Hb(II) in dilute solution (Figure 4C); and rapidly deoxygenated Hb(II) bound to CDB3 (Figure 4D). The experimental data are represented by symbols. The dashed lines represent model simulation results (see the Theoretical Section below). The dashed lines do not represent computer generated fits of the data.

It is apparent that predeoxygenated Hb(II) reacts at a slower rate with NO_2^- than does Hb(II) generated by rapid deoxygenation, both for hemoglobin in solution and for

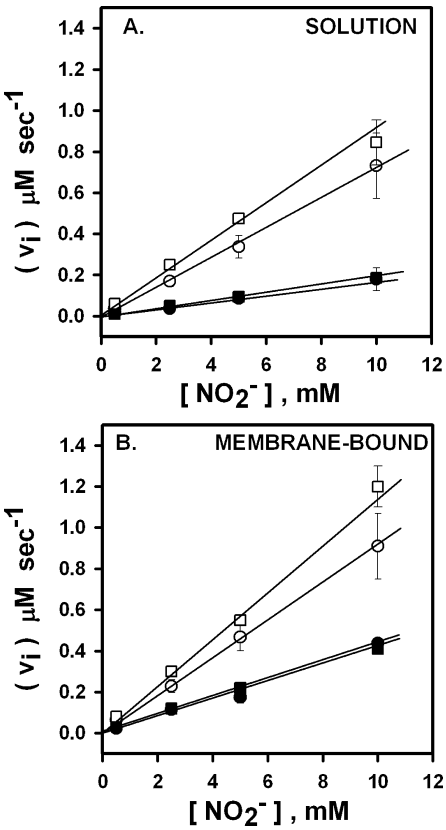

FIGURE 5: Plots of the initial velocity (v_i) vs [NO_2^-] for the reaction of NO_2^- with Hb(II). NO_2^- was reacted with predeoxygenated or rapidly deoxygenated hemoglobin in solution (A) or bound to the cytoplasmic domain of band 3 (CDB3) (B). The results represented by the circles came from experimental determinations. Open circles were from rapid deoxygenation experiments, while closed circles were from predeoxygenation experiments. The results represented by the squares were from model simulation studies. Open squares were from rapid deoxygenation simulations, while closed squares were from predeoxygenation simulations. The experimental reactions were performed as described in the legend to Figure 4, and the initial velocities were calculated as described in the text. Quantitative values for the slopes of the lines in this figure are given in Table 1.

hemoglobin bound to CDB3 (note the differences in time scales in Figure 4). The reaction of CDB3-bound predeoxygenated Hb(II) (Figure 4B) is faster than predeoxygenated Hb(II) in solution (Figure 4A). In contrast, rapidly deoxygenated membrane-bound Hb(II) (Figure 4D) reacted only slightly faster than rapidly deoxygenated Hb(II) in dilute solution (Figure 4C).

In order to quantitate the apparent differences in reactivity toward NO_2^- shown in Figure 4, the initial velocities were calculated for the loss of Hb(II) at 430 nm, as described in the Materials and Methods section. Initial linearity was established to a high degree of confidence over the first 30% of the reaction time course, as judged by the statistics associated with the linear fits indicated by the standard errors shown in Figure 5. In Figure 5A and B, the experimental results are presented as circles (rapid deoxygenation, open circles; predeoxygenation, closed circles). Table 1 lists the slopes of the lines in Figure 5. The squares represent the initial velocities taken from the simulation studies to be described below. The experimental results show that CDB3-bound predeoxygenated Hb(II) reacted 2.5-fold faster than predeoxygenated Hb(II) in solution, under otherwise identical conditions (Table 1). However, when the rapid deoxygenation method is used, there is a much smaller (~24%), but still significant, difference between CDB3-bound hemoglobin and hemoglobin in solution (Table 1). Nevertheless, it is apparent that the reaction of Hb(II) generated by the rapid deoxygenation method is faster than the reaction of predeoxygenated Hb(II), whether this comparison is made for hemoglobin in solution or for hemoglobin bound to CDB3 (Figure 5 and Table 1).

Theoretical Studies. There are two issues which need to be considered in order to properly interpret the nitrite reductase reaction of Hb(II) measured in dilute solutions with dithionite present. First, with regard to the use of dithionite, it is necessary to have a detailed understanding of the system of reactions that take place in the rapid deoxygenation experiment, where ~270 μM of dissolved O_2 is present initially. Molecular O_2 is rapidly reduced by dithionite to O_2^- (*45, 46*) during the rapid deoxygenation experiment. The O_2^- and its products then become involved in various side reactions with NO, dithionite, and hemoglobin, which in combination may challenge intuitive expectations for the effect of these various side reactions on the observed kinetics. Fortunately, all of the relevant kinetic reactions have been studied, and the values of the associated kinetic constants are available in the literature, thus supporting the feasibility of a model simulation study.

The second important issue to consider from a theoretical point of view concerns the role of hemoglobin dimer−tetramer association−dissociation kinetics when studying reactions involving liganded hemoglobin in dilute solutions. The observation of faster reaction kinetics in the rapid deoxygenation experiment is consistent with the predominance of R-state deoxy hemes, yet in the experimental section of this article, it was pointed that all of the Hb(II)O_2 was deoxygenated within ~50 ms and thus should have reacted with NO_2^- as slowly as predeoxygenated hemoglobin.

One hypothesis to explain such behavior is to propose that deoxy Hb(II) $\alpha\beta$ dimers predominate during the rapid deoxygenation experiment measured in solution. At the concentration of hemoglobin used in this study, ~63% of the Hb(II)O_2 would exist as $\alpha\beta$ dimers at pH 6.5 (*28*). Furthermore, deoxy Hb(II) $\alpha\beta$ dimers are expected to have R-state-like kinetics, where NO_2^- would react rapidly compared to T-state predeoxygenated Hb(II) tetramers (*49*). In addition, Hb(II)O_2 binds to CDB3 as $\alpha\beta$ dimers and remains in the fast reacting dimeric state when rapidly deoxygenated (*23, 27, 28*). Predeoxygenated hemoglobin will be entirely tetrameric both in solution (*50*) and when bound to CDB3 (*23, 27, 28*). The question to address is whether the deoxy R-state $\alpha\beta$ dimer would have a sufficiently long lifetime under the present experimental conditions, to react rapidly with NO_2^- (*49*). If the lifetime of R-state deoxy $\alpha\beta$ dimers was short relative to the reaction with NO_2^-, rapid deoxygenation and predeoxygenation kinetics should show identical kinetics.

Simulation of the Effect of O_2^- and Various Side Reactions on the Kinetics of Reaction of Hb(II) with NO_2^-. The Model.

The basic model used for this simulation is as follows:

$$\mathrm{Hb(II)} + \mathrm{NO_2^-} \leftrightarrow [\mathrm{Hb(II)NO_2^-}] \quad k_2, k_3 \qquad (2)$$

$$[\mathrm{Hb(II)NO_2^-}] \rightarrow \mathrm{Hb(III)} + \text{“}\mathrm{NO_2^{2-}}\text{”} \quad k_4 \qquad (3)$$

Table 1: Experimental and Theoretical Values Associated with the Data in Figure 5

reaction mechanism	experimental slope[a] from v_i vs $[NO_2^-]$ plot $\times 10^{-6}$, s^{-1}	simulated slope[a] from v_i vs $[NO_2^-]$ plot $\times 10^{-6}$, s^{-1}	simulation constants
pre-deoxygenation	solution	solution	solution
	17.8 ± 1.0	18.4 ± 0.2	$k_2 = 4.2\ M^{-1}\ s^{-1}$
			$k_3 = 3 \times 10^{-4}\ s^{-1}$
$Hb(II) + NO_2^- \overset{k_2}{\underset{k_3}{\leftrightarrow}} [Hb(II)NO_2^-] \overset{k_4}{\rightarrow} Hb(III) + NO$			$k_4 = 100\ s^{-1}$
			$k_3/k_2 = 71\ \mu M$
	membrane-bound	membrane-bound	membrane bound
	43.8 ± 3.6	39 ± 1.0	$k_2 = 12.5\ M^{-1}\ s^{-1}$
			$k_3 = 1.4 \times 10^{-4}\ s^{-1}$
			$k_4 = 30\ s^{-1}$
			$k_3/k_2 = 11\ \mu M$
rapid deoxygenation[b]	solution	solution	solution
	73.4 ± 2.2	82.2 ± 4.0	$k_2 = 25\ M^{-1}\ s^{-1}$
			$k_3 = 3 \times 10^{-4}\ s^{-1}$
			$k_4 = 65\ s^{-1}$
			$k_3/k_2 = 12\ \mu M$
	membrane-bound	membrane-bound	membrane bound
$Hb(II)(O_2) \overset{k_d}{\rightarrow} Hb(II)$	90.8 ± 1.2	118 ± 5.0	$k_2 = 30\ M^{-1}\ s^{-1}$
$Hb(II) + NO_2^- \overset{k_2}{\underset{k_3}{\leftrightarrow}} [Hb(II)NO_2^-] \overset{k_4}{\rightarrow} Hb(III) + NO$			$k_3 = 3.6 \times 10^{-4} s^{-1}$
			$k_4 = 78\ s^{-1}$
			$k_3/k_2 = 11\ \mu M$

[a] Mean and standard error. [b] k_d was determined experimentally (see Table 4 and Results).

In the simulation, NO was substituted for NO_2^{2-} since the NO_2^- reduction product NO_2^{2-} is known to rapidly form NO and water in subsequent reactions (*51*).

The basic model represented by eqs 2 and 3 differs from the models presented by Doyle et al. (*51*) and Huang et al. (*49*) in two respects. First, it does not include the reaction of Hb(II) with nitrous acid [Hb(II) + HONO → Hb(III) + NO + OH^-]. I have performed extensive model simulation studies that included the HONO reaction step using initial HONO concentrations ranging from 2.23 to 44.5×10^{-7} M, consistent with the p*K* for HONO (*51*) and the pH used in the experiment of interest (pH 6.5). I obtained virtually identical time courses when $k_{HONO} = 1.23 \times 10^4\ M^{-1}\ s^{-1}$ (*51*), and $k_2 = 25\ M^{-1}\ s^{-1}$, $k_3 = 3 \times 10^{-4}\ s^{-1}$, and $k_4 = 65\ s^{-1}$ (Table 1). Raising the value of the HONO rate constant 5-fold to reflect R-state Hb(II) reactivity (*49*) ($k_{HONO} = 6.15 \times 10^4\ M^{-1}\ s^{-1}$) resulted in a slightly faster time course at 10 mM sodium nitrite concentration. Thus, at the concentration of HONO present under our experimental conditions and given the literature values of k_{HONO} (*51*), the reaction of deoxy Hb(II) with NO_2^- virtually completely dominates the kinetics.

The second manner by which the model consisting of eqs 2 and 3 differs from the models of Doyle et al. (*51*) and Huang et al. (*49*) is on the introduction of the intermediate species [$Hb(II)NO_2^-$] (eq 2). I have found that use of a simple second order reaction scheme or even two parallel second order reactions (one for NO_2^- and one for HONO) did not adequately simulate the initial linearity observed in the kinetic time courses of Figure 1 (A and B). This suggests that some type of reversible intermediate may form during the reaction, associated with the initial binding of NO_2^- within the heme pocket prior to chemical reaction at the heme iron. Evidence was presented in Figure 1C for a spectral-kinetic heterogeneity in the overall reaction, which could be consistent with formation of such an intermediate, although other explanations are possible for that type of behavior.

Figure 6 shows the basic reductase mechanism (eqs 2 and 3) as well as side reactions, which directly relate to the basic mechanism within the context of the rapid deoxygenation experiment, where $Hb(II)O_2$ is mixed with NO_2^- and dithionite simultaneously. The values of the rate constants used for the reaction in Figure 6 and for other side reactions not shown in Figure 6 were taken from the literature (*7, 20, 41, 45, 46, 49, 52–66*), or they were determined in the simulation (k_2, k_3, and k_4) and are all listed in Tables 1−4.

NO_2^- Concentration Dependence. The theoretical time courses generated from the model simulation studies are shown as dashed curves in Figure 4. The values of the simulation constants k_2, k_3, and k_4 used to generate each time course are given in Table 1. The values of k_2, k_3, and k_4 were determined by trial and error, in order to generate the theoretical time courses in Figure 4. The simulated time

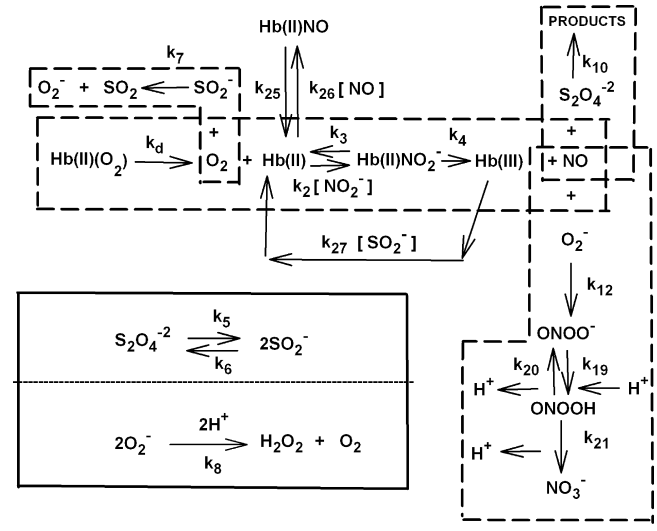

FIGURE 6: A simplified schematic diagram of the major reaction steps considered in model simulation studies involving side reactions in the rapid deoxygenation experiment. The main reaction involves rapid deoxygenation of $Hb(II)O_2$ by addition of dithionite ($S_2O_4^{-2}$) to yield Hb(II), with the dithionite monomer (SO_2^-) acting to scavenge O_2. NO_2^- then reacts with Hb(II) to form a reversible intermediate complex, which then yields Hb(III) and NO (see the text for complete details). These reactions and others were included in the simulation and are all listed in Tables 1−4.

Table 2: Non-Heme Reactions of Dithionite

$S_2O_4^{-2} \underset{k_6}{\overset{k_5}{\leftrightarrow}} 2\,SO_2^-$	$k_5 = 1.7\ s^{-1}$	$k_6 = 1.2 \times 10^9\ M^{-1}\ s^{-1}$	45
$SO_2^- + O_2 \overset{k_7}{\rightarrow} SO_2 + O_2^-$		$k_7 = 1.0 \times 10^8\ M^{-1}\ s^{-1}$	46
$2H^+ + 2O_2^- \overset{k_8}{\rightarrow} H_2O_2 + O_2$		$k_8 = 6.4 \times 10^9\ M^{-1}\ s^{-1}$ enzymatic value	52
$H_2O_2 + SO_2^- \overset{k_9}{\rightarrow}$ Products		$k_9 = 260\ M^{-1}\ s^{-1}$	46

courses in Figure 4, panels B−D, reproduced the experimental time courses to a high level, as judged visually by the fact that the simulations matched the experimental data over the entire reaction time courses. The simulated reactions of NO_2^- with predeoxygenated Hb(II) in solution (Figure 4A) are somewhat displaced at the highest concentration of NO_2^-.

Figure 5A and B (open and closed squares) shows plots of the initial velocities for the simulated time courses in Figure 4 (dashed curves) versus of NO_2^-. The initial velocities determined from the theoretical time courses in Figure 4 were comparable to the initial velocities obtained from the experimental time courses as illustrated in Figure 5, and quantitatively established in Table 1, where the slopes of the experimental and simulated lines in Figure 5 can be compared directly.

Table 1 also gives calculated values for the initial binding constant (k_3/k_2) for each type of experiment. These comparisons show that the initial affinity of NO_2^- for predeoxygenated Hb(II) in solution is ~6-fold lower than the affinity of Hb(II) generated by rapid deoxygenation in solution (Table 1). Predeoxygenation and rapid deoxygenation of hemoglobin bound to CDB3, both showed high initial affinity for the binding of NO_2^- compared to predeoxygenated Hb(II) in solution (Table 1).

Simulation Results for the Effect of the Superoxide Dismutation Reaction on the Kinetics of Hb(II)NO Formation. The results of the model simulation studies presented in Figures 4 and 5 could adequately represent the experimental findings when the value of k_8 was equal to the enzymatic rate constant for superoxide dismutation ($k_8 = 6.4 \times 10^9\ M^{-1}\ s^{-1}$) (Table 2). To test for the effect of O_2^- on the kinetics, I performed model simulations studies investigating the effect of variation in k_8. Figure 7 shows plots of the time courses for selected molecular species in Figure 6, generated from the simulation of the rapid deoxygenation of Hb(II)O_2, using a very small value of k_8 ($1 \times 10^{-4}\ M^{-1}\ s^{-1}$). Figure 7A, shows that a lag period occurs for the loss of Hb(II) and for the appearance of Hb(II)NO that lasts for about 800 s (the first 600 s are not shown). After the lag, Hb(II) decays, and Hb(II)NO appears with the same kinetics. Thus, under the rapid deoxygenation experimental conditions used in Figure 4, failure to consume O_2^- rapidly does not slow the NO_2^- reductase reaction, but rather delays its initiation.

Figure 7B−D illustrates the molecular basis for this lag period. There is a clear correlation between the length of the lag period and the decrease in NO_2^- and O_2^- concentrations and also in the appearance of NO_3^-. When O_2^- is completely consumed (Figure 7D), NO_2^- consumption (Figure 7B) and the appearance of NO_3^- (Figure 7C) both stop simultaneously. Changing k_8 from the enzymatic value of $6.4 \times 10^9\ M^{-1}\ s^{-1}$ to the nonenzymatic value appropriate for the experimental conditions given in the legend to Figure 4 ($k_8 = 1.3 \times 10^6\ M^{-1}\ s^{-1}$) (*52*) caused a very slight lag period lasting about 2 s, and the initial velocity for the reaction after that lag was actually ~25% faster than that determined when the enzymatic value of k_8 was used. Lowering the k_8 values further ($k_8 = 1 \times 10^5\ M^{-1}\ s^{-1}$, $1 \times 10^4\ M^{-1}\ s^{-1}$, and $1 \times 10^3\ M^{-1}\ s^{-1}$) significantly increased the lag time, but did not change the apparent rate constant after the lag period, beyond that reached when $k_8 = 1.3 \times 10^6\ M^{-1}\ s^{-1}$ (results not shown).

Since there was no evidence in the experimental section of this article for a lag comparable even to the small one seen when $k_8 = 1.3 \times 10^6\ M^{-1}\ s^{-1}$ (nonenzymatic dismutation at pH 6.5) (*52*), I conclude that the reaction of O_2^- with NO is not occurring to a significant degree because the O_2^- concentration is kept very low by the background dismutation rate occurring at pH 6.5 (*52*) and by the probable existence of superoxide dismutase in the dialyzed hemolysate. Furthermore, I conclude that during the lag period, the basic reductase mechanism consumes more NO_2^- than is consistent with stoichiometric expectations because Hb(III) is recycled back to Hb(II) due to the presence of dithionite (k_{27}) (Figure 6) and the virtual absence of NO consequent to its rapid reaction with O_2^- (k_{12}) (Figure 6). As the value of k_8 increases, O_2^- is consumed more rapidly, and free NO appears sooner and reacts with Hb(II) to form Hb(II)NO, which terminates the overall process, thus consuming less NO_2^- and producing less NO_3^- (Figure 6).

Effect of Hemoglobin Dimer−Tetramer Association−Dissociation Kinetics on the Kinetics of Reaction of Hb(II) with NO_2^-. The Model. Table 5 presents a rapid deoxygenation model containing the basic steps involved in the reaction of NO_2^- with the deoxy Hb(II) $\alpha\beta$ dimers and tetramers, the formation of Hb(II)NO, and the self-association of both unliganded and liganded $\alpha\beta$ dimers. This model was simplified by considering that (a) the reactions at the α and β subunits are equivalent, (b) the values of dimer−tetramer association−dissociation kinetic constants are independent of the type of ligand bound to the heme, and (c) by treating the reaction of deoxy T-state $\alpha_2\beta_2$ tetramers within the context of a simple sequential Adair-type scheme (*1*). In the Adair scheme used in Table 5, tetramers were assumed to switch to the T-state once the third liganded heme forms, allowing the last ligation step to have R-state kinetics (*33*). This change in the kinetic constants for the reaction with NO_2^- can be seen in Table 5 for steps (k_{48}, k_{49}) through (k_{54}, k_{55}) for NO_2^- binding, and steps (k_{99}, k_{100}) through (k_{105}, k_{106}) for NO binding. Note that for NO_2^- binding, the on kinetic constant was assumed to reflect the allosteric transition from the T-state to the R-state. In contrast, the on kinetic constant for NO binding to hemoglobin is known to be invariant, with the off kinetic constants accounting for cooperativity (*7*).

The values of k_2, k_3, and k_4 for the NO_2^- reductase reaction were taken from the simulation results of Table 1 for the rapid deoxygenation experiment for hemoglobin in solution. The values of the same constants for the T-state species were taken from the results from the predeoxygenation simulation results given in Table 1. The values of the association and dissociation kinetic constants for liganded R-state hemoglobin [Hb(II)O_2, Hb(II)NO_2^-, Hb(III), and Hb(II)NO] [(k_{34}, k_{35}), (k_{56}, k_{57}), (k_{69}, k_{70}), and (k_{89}, k_{90}) of Table 5] were all assumed to have the same values. The numbers used were derived

Table 3: Non-Heme Reactions of Nitric Oxide (NO)

$NO + S_2O_4^{-2} \xrightarrow{k_{10}}$ Products		$k_{10} = 1.4 \times 10^3\ M^{-1}\ s^{-1}$	7
$2NO + O_2 \xrightarrow{k_{11}} 2NO_2$		$k_{11} = 2.1 \times 10^6\ M^{-2}\ s^{-1}$	53, 54
$NO + O_2^- \xrightarrow{k_{12}} ONOO^-$		$k_{12} = 6.7 \times 10^9\ M^{-1}\ s^{-1}$	55
$N_2O_3 \underset{k_{14}}{\overset{k_{13}}{\leftrightarrow}} NO + NO_2$	$k_{13} = 4.3 \times 10^6\ s^{-1}$	$k_{14} = 1.1 \times 10^9\ M^{-1}\ s^{-1}$	54
$N_2O_3 + H_2O \underset{k_{16}}{\overset{k_{15}}{\leftrightarrow}} 2NO_2^- + 2H^+$	$k_{15} = 1.6 \times 10^3\ s^{-1}$	$k_{16} = 5.6\ M^{-1}\ s^{-1}$	54
$N_2O_3 + P_i \xrightarrow{k_{17}} P_iNO + NO_2^-$		$k_{17} = 6.4 \times 10^5\ M^{-1}\ s^{-1}$	54
$N_2O_3 + RSH \xrightarrow{k_{18}} RSNO + NO_2^- + H^+$		$k_{18} = 3.4 \times 10^7\ M^{-1}\ s^{-1}$ (R-state only)	56
$ONOO^- + H^+ \underset{k_{20}}{\overset{k_{19}}{\leftrightarrow}} ONOOH$	$k_{20} = 3.2 \times 10^3\ s^{-1}$	$k_{19} = 2 \times 10^{10}\ M^{-1}\ s^{-1}$	57
$ONOOH \xrightarrow{k_{21}} NO_3^- + H^+$	$k_{21} = 1.3\ s^{-1}$		58
$ONOO^- + NO \xrightarrow{k_{22}} NO_2 + NO_2^-$		$k_{22} = 4.5 \times 10^5\ M^{-1}\ s^{-1}$ (model-dependent value)	59

Table 4: Non-Model Dependent Reactions at the Heme

$Hb(II)(O_2) \xrightarrow{k_d} Hb(II)$	$k_d = 59\ s^{-1}$		41
$Hb(II)(O_2) + NO \xrightarrow{k_{23}} Hb(III) + ONOO^-$		$k_{23} = 7 \times 10^7\ M^{-1}\ s^{-1}$	60, 61
$Hb(II) + NO_2 \xrightarrow{k_{24}} Hb(III) + NO_2^-$		$k_{24} = 1 \times 10^9\ M^{-1}\ s^{-1}$	49
$Hb(II)(NO) \underset{k_{26}}{\overset{k_{25}}{\leftrightarrow}} Hb(II) + NO$	T-state $k_{25} = 1 \times 10^{-3}\ s^{-1}$ R-state $k_{25} = 9.5 \times 10^{-6}\ s^{-1}$	$k_{26} = 2.4\ x10^7\ M^{-1}\ s^{-1}$	7, 20
$Hb(III) + SO_2^- \xrightarrow{k_{27}} Hb(II)$		$k_{27} = 6 \times 10^6\ M^{-1}\ s^{-1}$ (average of α and β chains)	62, 63
$Hb(III)(NO) \underset{k_{29}}{\overset{k_{28}}{\leftrightarrow}} Hb(III) + NO$	$k_{28} = 8.5\ s^{-1}$ (average of α and β chains)	$k_{29} = 7 \times 10^5\ M^{-1}\ s^{-1}$ (average of α and β chains)	64
$Hb(III)(NO_2^-) \underset{k_{31}}{\overset{k_{30}}{\leftrightarrow}} Hb(III) + NO_2^-$	$k_{30} = 0.4\ s^{-1}$ (average of α and β chains)	$k_{31} = 84\ M^{-1}\ s^{-1}$ (average of α and β chains)	65
$Hb(II)(O_2) + O_2^- \xrightarrow{k_{32}} Hb(III) + H_2O_2 + O_2$		$k_{32} = 4 \times 10^3\ M^{-1}\ s^{-1}$	66
$Hb(III) + O_2^- \xrightarrow{k_{33}} Hb(II)(O_2)$		$k_{33} = 6 \times 10^3\ M^{-1}\ s^{-1}$	66

from the measurements of Nagle and Gibson (*67*), who studied Hb(II)CO.

Model Simulation Studies for the Effect of Variation of the Dimer to Tetramer Association Rate Constant for deoxyHb(II) (k_{38}) on the Kinetics of NO_2^- Reaction with Hb(II) Generated by Rapid Deoxygenation of Hb(II)O_2. Figure 8 shows the simulation results calculated at three different values of k_{38} given in the legend and the same value of k_{39} given in Table 5. These simulations are shown in Figure 8 as the curved lines that lack data points (dotted, dash-dot-dash, and dashed). The experimental results in Figure 8 (closed and open circles) came from the rapid deoxygenation experiment (Figure 4C at 10 mM NO_2^-) and from the predeoxygenation experiment (Figure 4A, at 10 mM NO_2^-), respectively. When $k_{38} = 10^3-10^4\ M^{-1}\ s^{-1}$, the fraction of fast phase is equal to ~60%. This is equivalent to the amount of Hb(II)O_2 $\alpha\beta$ dimer present in the sample initially, as indicated above. Thus, the lifetime of the deoxy Hb(II) $\alpha\beta$ dimer is sufficiently long for NO_2^- to react with those dimers before they self-associate to deoxy tetramers. When $k_{38} = 10^5\ M^{-1}\ s^{-1}$, the fraction of slow phase increases from ~40% to ~50% of the total reaction, reflecting a larger dimer to tetramer self-association rate constant and the slower NO_2^- reductase activity of deoxy T-state tetramers. At $k_{38} = 1 \times 10^5\ M^{-1}\ s^{-1}$, the tetramer−dimer dissociation constant ($K_{4,2}$) for deoxy Hb(II) is equal to 3.5×10^{-13} M, given the value of k_{39} shown in Table 5. This value is within the range of constants determined experimentally by Chu and Ackers (*50*) at pH 6.5 and 25 °C, but at higher chloride concentration (0.1 M NaCl).

DISCUSSION

The experiments presented in this study were designed to determine the NO_2^- reductase activity of hemoglobin when it is bound in a complex with CDB3 at the inner surface of the erythrocyte membrane. Dithionite was used both to maintain anaerobicity when studying the reaction of T-state deoxy Hb(II) tetramers and to characterize the NO_2^- reductase reaction of Hb(II) when it is generated by rapidly mixing Hb(II)O_2 with dithionite and NO_2^- simultaneously. This comparison was of interest since earlier evidence had shown that Hb(II)O_2 binds to CDB3 as R-state $\alpha\beta$ dimers and is stabilized in the dimeric R-state immediately after rapid deoxygenation (*23, 28*).

The results showed that the rate of reaction of Hb(II) with NO_2^- was independent of dithionite concentration, thus indicating that dithionite does not reduce NO_2^- to NO directly. Furthermore, CDB3-bound predeoxygenated Hb(II) reacted about 2.5-fold faster than predeoxygenated Hb(II) in solution, while rapidly deoxygenated CDB3-bound Hb(II)O_2 reacted only ~23% faster than rapidly deoxygenated Hb(II)O_2 in dilute solution. However, rapidly deoxygenated Hb(II) reacted faster than predeoxygenated Hb(II), whether

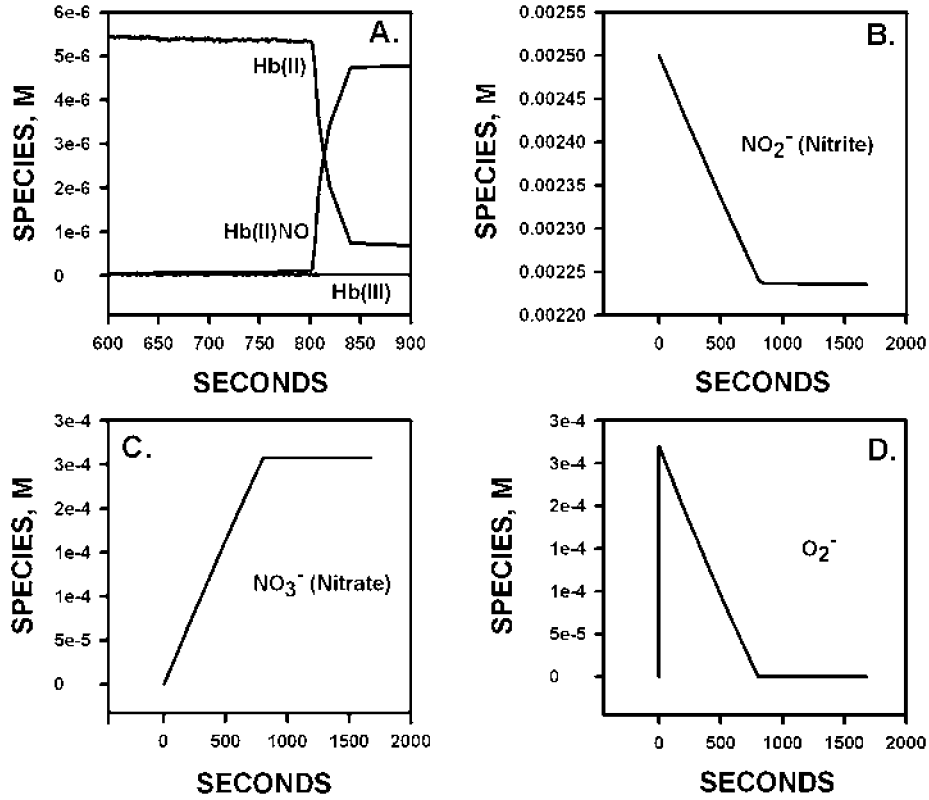

FIGURE 7: Model simulation for the rapid deoxygenation experiment in solution. The simulation conditions for the reactions were the same as in Figure 4C for 2.5 mM NO_2^-, except that an abnormally small value k_8 (1×10^{-4} M^{-1} s^{-1}) (Table 2) was used for the rate constant for superoxide dismutation. The values for the rate constants for the reductase part of the mechanism (Figure 6) were $k_2 = 25$ M^{-1} s^{-1}, $k_3 = 3 \times 10^{-4}$ s^{-1}, and $k_4 = 65$ s^{-1}. Panel A shows the development of an approximately 800 s lag period in the reaction of Hb(II) (the first 600 s of the simulation are not shown). There was an identical lag in the appearance of Hb(II)NO. There was no significant increase in Hb(III). This figure also shows that NO_2^- is lost (panel B), as NO_3^- forms (panel C), both with the same kinetics as is seen for the loss of O_2^- (panel D) after its initial, very rapid formation from the reduction of O_2 by dithionite (see Figure 6). Once all of the O_2^- is consumed, the NO generated by the reductase reaction reacts with Hb(II) to form Hb(II)NO as seen in panel A. What is not shown in this figure is that $ONOO^-$ does not change in concentration during the course of the reaction and that SO_2, the other product of the reaction of SO_2^- with O_2, increases rapidly with the formation of O_2^- but remains constant for the remainder of the reaction.

in solution or bound to CDB3. Thus, rapidly deoxygenated CDB3-bound Hb(II) reacted with NO_2^- 5-fold faster than predeoxygenated Hb(II) in solution.

What accounts for the difference in kinetics between the rapidly deoxygenated versus the predeoxygenated Hb(II) measured in solution? When attempting to answer this question, it is important to recall the evidence described above, indicating that Hb(II)O_2 was completely deoxygenated in the rapid deoxygenation experiment (±10%) compared to the kinetics of reaction of NO_2^- with predeoxygenated Hb(II). This finding suggests that Hb(II) confronted by NO_2^- should have reacted with the same kinetics, independent of the method employed for deoxygenating Hb(II)O_2. However, this was not the case. Model simulation studies on the role of side reactions involving O_2^- and the other reaction products (Table 2−4) indicated that the kinetic time courses observed in Figure 4C and D, were uncomplicated by side reactions. A relatively large quantity of O_2^- is generated in the rapid deoxygenation reaction due to the reduction of dissolved O_2 by dithionite. The theoretical work showed that lag periods are expected, not a slower reaction rate. Thus, the reaction of O_2^- with NO appears to be negligible since there was no lag period in the formation of Hb(II)NO (Figures 3 and 4), as would be expected on the basis of the theoretical studies if the superoxide dismutation reaction were not sufficiently fast (Figure 7). Indeed, the simulations showed that even nonenzymatic dismutation activity at pH 6.5 is sufficient to consume O_2^- rapidly enough to allow Hb(II)NO to form. Thus, it is most likely that the observed difference in reactivity between Hb(II) prepared by predeoxygenation versus rapid deoxygenation has to do with the fact that hemoglobin reactivity is controlled not only by the oxidation state of the heme iron, but also by hemoglobin's conformation.

The R-state of hemoglobin is known to react faster with NO_2^- compared to the T-state, both on the basis of studies with native hemoglobin (*49*) and studies using mutant and chemically modified hemoglobin (*68*). The kinetic studies of Crawford et al. (*68*) showed that blocking the β-93 −SH group with *N*-ethylmalaimide (NEM) increased the NO_2^- reductase reaction rate of deoxy Hb(II) ~6-fold. This is similar to the ~4-fold faster rate seen in the solution studies when the reaction of Hb(II) generated by rapidly deoxygenated R-state Hb(II)O_2 was compared to the reaction of predeoxygenated T-state Hb(II) (Table 1). Thus, it seems likely that the difference between the results for the rapid deoxygenation experiment versus the predeoxygenation experiment somehow reflects at least in part the difference in R-state reactivity (rapid deoxygenation) versus T-state reactivity (predeoxygenation).

The above considerations raise an important question. What factors are present in the rapid deoxygenation experiment which would maintain Hb(II) in the deoxy R-state long enough to react rapidly with NO_2^-? One factor considered

Table 5: Model for Hemoglobin Dimer−Tetramer Association− Dissociation Kinetics and the Nitrite Reductase Activity of Deoxy Hemoglobin

$2\alpha(O_2)\beta(O_2) \underset{k_{35}}{\overset{k_{34}}{\leftrightarrow}} \alpha_2(O_2)_2\beta_2(O_2)_2$	$k_{34} = 3.3 \times 10^5\ M^{-1}\ s^{-1}$	$k_{35} = 2.0\ s^{-1}$	67
$\alpha_2(O_2)_2\beta_2(O_2)_2 \overset{k_{36}}{\rightarrow} \alpha_2\beta_2$	$k_{36} = 59\ s^{-1}$		41
$\alpha(O_2)\beta(O_2) \overset{k_{37}}{\rightarrow} \alpha\beta$	$k_{37} = 59\ s^{-1}$		41
$2\alpha\beta \underset{k_{39}}{\overset{k_{38}}{\leftrightarrow}} \alpha_2\beta_2$	k_{38} = varies	$k_{39} = 3.5 \times 10^{-8}\ s^{-1}$	
$NO_2^- + \alpha\beta \underset{k_{41}}{\overset{k_{40}}{\leftrightarrow}} \alpha\beta(NO_2^-)$	$k_{40} = 25\ M^{-1}\ s^{-1}$	$k_{41} = 0.0003\ s^{-1}$	Table 1
$NO_2^- + \alpha\beta \underset{k_{43}}{\overset{k_{42}}{\leftrightarrow}} \alpha(NO_2^-)\beta$	$k_{42} = 25\ M^{-1}\ s^{-1}$	$k_{43} = 0.0003\ s^{-1}$	Table 1
$NO_2^- + \alpha\beta(NO_2^-) \underset{k_{45}}{\overset{k_{44}}{\leftrightarrow}} \alpha(NO_2^-)\beta(NO_2^-)$	$k_{44} = 25\ M^{-1}\ s^{-1}$	$k_{45} = 0.0003\ s^{-1}$	Table 1
$NO_2^- + \alpha(NO_2^-)\beta \underset{k_{47}}{\overset{k_{46}}{\leftrightarrow}} \alpha(NO_2^-)\beta(NO_2^-)$	$k_{46} = 25\ M^{-1}\ s^{-1}$	$k_{47} = 0.0003\ s^{-1}$	Table 1
$NO_2^- + \alpha_2\beta_2 \underset{k_{49}}{\overset{k_{48}}{\leftrightarrow}} \alpha_2(NO_2^-)\beta_2$	$k_{48} = 4.2\ M^{-1}\ s^{-1}$	$k_{49} = 0.0003\ s^{-1}$	Table 1
$NO_2^- + \alpha_2(NO_2^-)\beta_2 \underset{k_{51}}{\overset{k_{50}}{\leftrightarrow}} \alpha_2(NO_2^-)_2\beta_2$	$k_{50} = 4.2\ M^{-1}\ s^{-1}$	$k_{51} = 0.0003\ s^{-1}$	Table 1
$NO_2^- + \alpha_2(NO_2^-)_2\beta_2 \underset{k_{53}}{\overset{k_{52}}{\leftrightarrow}} \alpha_2(NO_2^-)_2\beta_2(NO_2^-)$	$k_{52} = 4.2\ M^{-1}\ s^{-1}$	$k_{53} = 0.0003\ s^{-1}$	Table 1
$NO_2^- + \alpha_2(NO_2^-)_2\beta_2(NO_2^-) \underset{k_{55}}{\overset{k_{54}}{\leftrightarrow}} \alpha_2(NO_2^-)_2\beta_2(NO_2^-)_2$	$k_{54} = 25\ M^{-1}\ s^{-1}$	$k_{55} = 0.0003\ s^{-1}$	Table 1
$2\alpha(NO_2^-)\beta(NO_2^-) \underset{k_{57}}{\overset{k_{56}}{\leftrightarrow}} \alpha_2(NO_2^-)_2\beta_2(NO_2^-)_2$	$k_{56} = 3.3 \times 10^5\ M^{-1}\ s^{-1}$	$k_{57} = 2\ s^{-1}$	67
$\alpha_2(NO_2^-)_2\beta_2(NO_2^-)_2 \overset{k_{58}}{\rightarrow} \alpha_2(met)_2\beta_2(met)_2 + 4NO$		$k_{58} = 100\ s^{-1}$	Table 1
$\alpha\beta(NO_2^-) \overset{k_{59}}{\rightarrow} \alpha\beta(met) + NO$		$k_{59} = 65\ s^{-1}$	Table 1
$\alpha(NO_2^-)\beta \overset{k_{60}}{\rightarrow} \alpha(met)\beta + NO$		$k_{60} = 65\ s^{-1}$	Table 1
$\alpha\beta(met) + NO_2^- \underset{k_{62}}{\overset{k_{61}}{\leftrightarrow}} \alpha(NO_2^-)\beta(met)$	$k_{61} = 25\ M^{-1}\ s^{-1}$	$k_{62} = 0.0003\ s^{-1}$	Table 1
$\alpha(met)\beta + NO_2^- \underset{k_{64}}{\overset{k_{63}}{\leftrightarrow}} \alpha(met)\beta(NO_2^-)$	$k_{63} = 25\ M^{-1}\ s^{-1}$	$k_{64} = 0.0003\ s^{-1}$	Table 1
$\alpha(NO_2^-)\beta(NO_2^-) \overset{k_{65}}{-} \alpha(NO_2^-)\beta(met) + NO$		$k_{65} = 65\ s^{-1}$	Table 1
$\alpha(NO_2^-)\beta(NO_2^-) \overset{k_{66}}{\rightarrow} \alpha(met)\beta(NO_2^-) + NO$		$k_{66} = 65\ s^{-1}$	Table 1
$\alpha(NO_2^-)\beta(met) \overset{k_{67}}{\rightarrow} \alpha(met)\beta(met) + NO$		$k_{67} = 65\ s^{-1}$	Table 1
$\alpha(met)\beta(NO_2^-) \overset{k_{68}}{\rightarrow} \alpha(met)\beta(met) + NO$		$k_{68} = 65\ s^{-1}$	Table 1
$2\alpha(met)\beta(met) \underset{k_{70}}{\overset{k_{69}}{\leftrightarrow}} \alpha_2(met)_2\beta_2(met)_2$	$k_{69} = 3.3 \times 10^5\ M^{-1}\ s^{-1}$	$k_{70} = 2\ s^{-1}$	67
$\alpha\beta(met) + SO_2^- \overset{k_{71}}{\leftrightarrow} \alpha\beta$	$k_{71} = 6 \times 10^6\ M^{-1}\ s^{-1}$		62, 63
$\alpha(met)\beta + SO_2^- \overset{k_{72}}{\leftrightarrow} \alpha\beta$	$k_{72} = 6 \times 10^6\ M^{-1}\ s^{-1}$		62, 63
$\alpha(NO_2^-)\beta(met) + SO_2^- \overset{k_{73}}{\leftrightarrow} \alpha(NO_2^-)\beta$	$k_{73} = 6 \times 10^6\ M^{-1}\ s^{-1}$		62, 63
$\alpha(met)\beta(NO_2^-) + SO_2^- \overset{k_{74}}{\leftrightarrow} \alpha\beta(NO_2^-)$	$k_{74} = 6 \times 10^6\ M^{-1}\ s^{-1}$		62, 63
$\alpha(met)\beta(met) + SO_2^- \overset{k_{75}}{\leftrightarrow} \alpha\beta(met)$	$k_{75} = 6 \times 10^6\ M^{-1}\ s^{-1}$		62, 63
$\alpha(met)\beta(met) + SO_2^- \overset{k_{76}}{\leftrightarrow} \alpha(met)\beta$	$k_{76} = 6 \times 10^6\ M^{-1}\ s^{-1}$		62, 63
$\alpha_2(met)_2\beta_2(met)_2 + SO_2^- \overset{k_{77}}{\rightarrow} \alpha_2(met)\beta_2(met)_2$	$k_{77} = 6 \times 10^6\ M^{-1}\ s^{-1}$		62, 63
$\alpha_2(met)\beta_2(met)_2 + SO_2^- \overset{k_{78}}{\rightarrow} \alpha_2\beta_2(met)_2$	$k_{78} = 6 \times 10^6\ M^{-1}\ s^{-1}$		62, 63
$\alpha_2\beta_2(met)_2 + SO_2^- \overset{k_{79}}{\rightarrow} + \alpha_2\beta_2(met)$	$k_{79} = 6 \times 10^6\ M^{-1}\ s^{-1}$		62, 63
$\alpha_2\beta_2(met) + SO_2^- \overset{k_{80}}{\rightarrow} \alpha_2\beta_2$	$k_{80} = 6 \times 10^6\ M^{-1}\ s^{-1}$		62, 63
$\alpha\beta + NO \underset{k_{82}}{\overset{k_{81}}{\leftrightarrow}} + \alpha(NO)\beta$	$k_{81} = 2.4 \times 10^7\ M^{-1}\ s^{-1}$	$k_{82} = 9.5 \times 10^{-6}\ s^{-1}$	7, 20
$\alpha\beta + NO \underset{k_{84}}{\overset{k_{83}}{\leftrightarrow}} \alpha\beta(NO)$	$k_{83} = 2.4 \times 10^7\ M^{-1}\ s^{-1}$	$k_{84} = 9.5 \times 10^{-6}\ s^{-1}$	7, 20
$\alpha(NO)\beta + NO \underset{k_{86}}{\overset{k_{85}}{\leftrightarrow}} \alpha(NO)\beta(NO)$	$k_{85} = 2.4 \times 10^7\ M^{-1}\ s^{-1}$	$k_{86} = 9.5 \times 10^{-6}\ s^{-1}$	7, 20
$\alpha\beta(NO) + NO \underset{k_{88}}{\overset{k_{87}}{\leftrightarrow}} \alpha(NO)\beta(NO)$	$k_{87} = 2.4 \times 10^7\ M^{-1}\ s^{-1}$	$k_{88} = 9.5 \times 10^{-6}\ s^{-1}$	7, 20
$2\alpha(NO)\beta(NO) \underset{k_{90}}{\overset{k_{89}}{\leftrightarrow}} \alpha_2(NO)_2\beta_2(NO)_2$	$k_{89} = 3.3 \times 10^5\ M^{-1}\ s^{-1}$	$k_{90} = 2\ s^{-1}$	67
$\alpha\beta(NO_2^-) + NO \underset{k_{92}}{\overset{k_{91}}{\leftrightarrow}} \alpha(NO)\beta(NO_2^-)$	$k_{91} = 2.4 \times 10^7\ M^{-1}\ s^{-1}$	$k_{92} = 9.5 \times 10^{-6}\ s^{-1}$	7, 20
$\alpha(NO_2^-)\beta + NO \underset{k_{94}}{\overset{k_{93}}{\leftrightarrow}} \alpha(NO_2^-)\beta(NO)$	$k_{93} = 2.4 \times 10^7\ M^{-1}\ s^{-1}$	$k_{94} = 9.5 \times 10^{-6}\ s^{-1}$	7, 20
$\alpha\beta(met) + NO \underset{k_{96}}{\overset{k_{95}}{\leftrightarrow}} \alpha(NO)\beta(met)$	$k_{95} = 2.4 \times 10^7\ M^{-1}\ s^{-1}$	$k_{96} = 9.5 \times 10^{-6}\ s^{-1}$	7, 20
$\alpha(met)\beta + NO \underset{k_{98}}{\overset{k_{97}}{\leftrightarrow}} \alpha(met)\beta(NO)$	$k_{97} = 2.4 \times 10^7\ M^{-1}\ s^{-1}$	$k_{98} = 9.5 \times 10^{-6}\ s^{-1}$	7, 20
$\alpha_2\beta_2 + NO \underset{k_{100}}{\overset{k_{99}}{\leftrightarrow}} \alpha_2(NO)\beta_2$	$k_{99} = 2.4 \times 10^7\ M^{-1}\ s^{-1}$	$k_{100} = 1 \times 10^{-3}\ s^{-1}$	7, 20
$\alpha_2(NO)\beta_2 + NO \underset{k_{102}}{\overset{k_{101}}{\leftrightarrow}} \alpha_2(NO)_2\beta_2$	$k_{101} = 2.4 \times 10^7\ M^{-1}\ s^{-1}$	$k_{102} = 1 \times 10^{-3}\ s^{-1}$	7, 20
$\alpha_2(NO)_2\beta_2 + NO \underset{k_{104}}{\overset{k_{103}}{\leftrightarrow}} \alpha_2(NO)_2\beta_2(NO)$	$k_{103} = 2.4 \times 10^7\ M^{-1}\ s^{-1}$	$k_{104} = 1 \times 10^{-3}\ s^{-1}$	7, 20
$\alpha_2(NO)_2\beta_2(NO) + (NO) \underset{k_{106}}{\overset{k_{105}}{\leftrightarrow}} \alpha_2(NO)_2\beta_2(NO)_2$	$k_{105} = 2.4 \times 10^7\ M^{-1}\ s^{-1}$	$k_{106} = 9.5 \times 10^{-6}\ s^{-1}$	7, 20

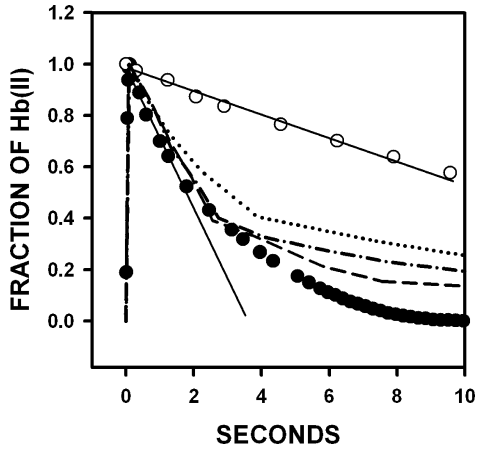

FIGURE 8: Comparison of experimental and theoretical time courses for the reaction of NO_2^- with Hb(II). The theoretical curves (no data points) were generated by the model given in Table 5. The experimental results for the rapid deoxygenation experiment (●) came from Figure 4 C ($[NO_2^-] = 10$ mM), and those for the predeoxygenation experiment (○) came from Figure 4 A ($[NO_2^-] = 10$ mM). The initial conditions used in the simulation of the model in Table 5 were as follows: $[NO_2^-] = 10$ mM; [Hb(II)O_2 tetramer] = 0.503 μM; [Hb(II)O_2 dimer] = 1.74 μM; $[S_2O_4^{-2}] = 5$ mM, and $[SO_2^{-1}] = 2.6$ μM. The fraction of Hb(II) was determined as described in the legend to Figure 4. The theoretical curves were generated using the following values for k_{38}: (dotted curve) = 1×10^5 M^{-1} s^{-1}, (dash-dot-dash curve) = 1×10^4 M^{-1} s^{-1}, and (dashes only curve) = 1×10^3 M^{-1} s^{-1}. The value of k_{39} was held constant and is given in Table 5

was the lifetime of the R-state deoxy $\alpha\beta$ dimer (Table 5 and Figure 8). There is about 63% Hb(II)O_2 $\alpha\beta$ dimer present in solution prior to initiation of the rapid deoxygenation reaction. Fast reacting deoxy R-state $\alpha\beta$ dimers are expected to self-associate to slow reacting T-state tetramers. This issue was explored using the model given in Table 5, with results shown in Figure 8. Those results indicated that reaction of deoxy R-state $\alpha\beta$ dimers dominate the initial 50% to 60% of the reaction, with the percentage depending on the value of k_{38} that was used.

One other factor that may play a role in stabilizing the R-state in the rapid deoxygenation experiment is the formation of SNO hemoglobin by nitrosation of the β-93 −SH group. There is clear evidence that covalent modification of the β-93 −SH group of Hb(II)O_2 leads to modified hemoglobin stabilized with R-state reactivity toward NO_2^- (*68, 69*). There is also direct evidence that nitrosation of the β-93 −SH group increases the oxygen affinity of hemoglobin (*70*), presumably also by R-state stabilization. SNO hemoglobin can from under anaerobic conditions, presumably involving a nitrite reduction intermediate with electron delocalization expanded to include the β-93 −SH group of Hb(II) (*71, 72*). However, to explain the difference in reactivity between the rapid deoxygenation experiment and the predeoxygenation experiment, some additional process would have to also be proposed to allow for faster formation of SNO-related stabilization of the R-state by Hb(II) generated by rapid deoxygenation versus the T-state deoxy hemes of predeoxygenated Hb(II).

Another question to ask is by what mechanism does CDB3-bound predeoxygenated Hb(II) react faster than predeoxygenated Hb(II) in solution (Table 1)? In both cases, hemoglobin should exist entirely within the tetrameric T-state (*23, 28*). One possible explanation is based on recent experimental evidence indicating that IHP binding to the 2,3-DPG site within the central cavity of the T-state Hb(II) tetramer alters the rate of NO_2^- reactivity in the sol−gel experiment (*73*). In that experiment, the T-state quaternary structure is stabilized by the sol−gel matrix, implying that the functional changes occur within the T-state. Thus, deoxy Hb(II) tetramer binding to CDB3 alters NO_2^- reactivity within the T-state, causing a faster NO_2^- reductase reaction.

The experimental results of this article support the view that rapid generation of NO by CDB3-bound hemoglobin may increase the probability of NO release from the red cell. Whether the effect observed in this study applies to the intact red cell is an important and difficult question to answer. As outlined in the introduction, some studies suggest that Hb(II) has a higher affinity for CDB3 than does Hb(II)O_2, while other equally valid studies indicate that Hb(II)O_2 has the higher affinity. The evidence suggests that Hb(II)O_2 $\alpha\beta$ dimers bind to CDB3 (*23, 28*). Given the very high concentration of hemoglobin within the erythrocyte, a value of $K_{4,2}$ equal to 3 μM was shown to yield as much as 100 μM $\alpha\beta$ Hb(II)O_2 dimers (*23*). This is enough dimer to cover all copies of band 3 on the membrane. CDB3-bound Hb(II)O_2 $\alpha\beta$ dimers should be expected to deoxygenate prior to deoxygenation of intracellular Hb(II)O_2. In that case, there should be little or no competition with Hb(II) initially, if the concentration of Hb(II) is smaller than Hb(II)O_2 $\alpha\beta$ dimers within the fully oxygenated erythrocyte. However, it is not clear whether these two forms of hemoglobin actually bind to the same site on CDB3. Cassoly (*28*) found two types of complexes in centrifugation studies using Hb(II)O_2. One complex contained the equivalent of one Hb(II)O_2 tetramer per dimer of CDB3 (i.e., one $\alpha\beta$ hemoglobin dimer per CDB3 subunit), and the other contained two Hb(II)O_2 tetramers per CDB3 dimer. Cassoly suggested that there are two binding sites for the $\alpha\beta$ Hb(II)O_2 dimer per CDB3 subunit, but only one mutually exclusive Hb(II)O_2 tetramer binding site (*28*). This is an interesting suggestion since it is not clear how an Hb(II)O_2 tetramer can bind to CDB3 when accessibility to the 2,3-DPG site is blocked within the R-state tetramer. Two allosterically interacting sites could account for apparent mutual exclusivity in Hb(II)O_2 binding to CDB3. Indeed, in later studies, Salhany and Cassoly (*35*) found clear evidence for long distant conformational changes within the CDB3 dimer upon binding of Hb(II)O_2. Furthermore, recent studies have suggested that residues 12−23 of CDB3 constitute the high affinity site for Hb(II) (*74*), while earlier crystallographic studies showed that the CDB3 fragment containing amino acid residues 1−11 cocrystallized at the 2,3-DPG binding site (*29*). Residues 1−11 apparently can affect the affinity of hemoglobin binding to residues 12−23 by some mechanism (*74*). Further studies of the mechanism of liganded and unliganded hemoglobin binding to CDB3 seem necessary.

ACKNOWLEDGMENT

I thank Dr. Larry Schopfer for reading the manuscript and for discussions.

REFERENCES

1. Antonini, E., and Brunori, M. (1971) *Hemoglobin and Myoglobin in Their Reactions with Ligands, Frontiers in Biology* (Neuberger, A., and Tatum, E. L., Eds.) *Vol. 21*, North-Holland Publishing Company, Amsterdam.

2. Cassoly, R. (1974) Relation between optic absorption spectrum and structure of nitrosyl hemoglobin. *C.R. Acad. Sci. Hebd. Seances Acad. Sci. D 278*, 1417–1420.
3. Salhany, J. M. (1974) Ultraviolet circular dichroism of nitrosyl hemoglobin. *FEBS Lett. 49*, 84–86.
4. Salhany, J. M., Ogawa, S., and Shulman, R. G. (1974) Spectral-kinetic heterogeneity in reactions of nitrosyl hemoglobin. *Proc. Natl. Acad. Sci. U.S.A. 71*, 3359–3362.
5. Salhany, J. M., Ogawa, S., and Shulman, R. G. (1975) Correlation between quaternary structure and ligand dissociation kinetics for fully liganded hemoglobin. *Biochemistry 14*, 2180–2190.
6. Perutz, M. F., Kilmartin, J. V., Nagai, K., Szabo, A., and Simon, S. R. (1976) Influence of globin structure on the state of the heme. Ferrous low spin derivatives. *Biochemistry 15*, 378–387.
7. Moore, E. G., and Gibson, Q. H. (1976) Cooperativity in the dissociation of nitric oxide from hemoglobin. *J. Biol. Chem. 251*, 2788–2794.
8. Monod, J., Wyman, J., and Changeux, J.-P. (1965) On the nature of allosteric transitions: A plausible model. *J. Mol. Biol. 12*, 88–118.
9. Furchgott, R. F., and Zawadzki, J. V. (1980) The obligatory role of endothelial cells in the relaxation of arterial smooth muscle by acetylcholine. *Nature 288*, 373–376.
10. Ignarro, L. J., Buga, G. M., Wood, K. S., Byrns, R. E., and Chaudhuri, G. (1987) Endothelium-derived relaxing factor produced and released from artery and vein is nitric oxide. *Proc. Natl. Acad. Sci. U.S.A. 84*, 9265–9269.
11. Ignarro, L. J., Byrns, R. E., Buga, G. M., and Wood, K. S. (1987) Endothelium-derived relaxing factor from pulmonary artery and vein possesses pharmacologic and chemical properties identical to those of nitric oxide radical. *Cric. Res. 61*, 866–879.
12. Palmer, R. M., Aston, D. S., and Moncada, S. (1988) Vascular endothelial cells synthesize nitric oxide from L-arginine. *Nature 333*, 664–666.
13. Palmer, R. M., Ferrige, A. G., and Moncada, S. (1987) Nitric oxide release accounts for the biological activity of endothelium-derived relaxing factor. *Nature 327*, 524–526.
14. Ellsworth, M. L., Forrester, T., Ellis, C. G., and Dietrich, H. H. (1995) The erythrocyte as a regulator of vascular tone. *Am. J. Physiol. 269*, H2155-H2161.
15. Dietrich, H. H., Ellsworth, M. L., and Sprague, R. S., Jr (2000) Red blood cell regulation of microvascular tone through adenosine triphosphate. *Am. J. Physiol. Heart Circ. Phys. 278*, H1294−H1298.
16. Jia, L., Bonaventura, C., Bonaventura, J., and Stamler, J. S. (1996) S-nitrosohaemoglobin: a dynamic activity of blood involved in vascular control. *Nature 380*, 221–226.
17. Cosby, K., Partovi, K. S., Crawford, J. H., Patel, R. P., Reiter, C. D., Martyr, S., Yang, B. K., Waclawiw, M. A., Zalos, G., Xu, X., Huang, K. T., Shields, H., Kim-Shapiro, D. B., Schechter, A. N., Canno, R. O., III, and Gladwin, M. T. (2003) Nitrite reduction to nitric oxide by deoxyhemogloin vasodilates the human circulation. *Nat. Med. 9*, 1498–1505.
18. Nagababu, E., Ramasamy, S., Abernethy, D. R., and Rifkind, J. M. (2003) Active nitric oxide produced in the red cell under hypoxic conditions by deoxyhemoglobin mediated nitrite reduction. *J. Biol. Chem. 278*, 46349–46356.
19. Gladwin, M. T., Raat, N. J. H., Shiva, S., Dezfulian, C., Hogg, N., Kim-Shapiro, R. P., and Patel, D. B. (2006) Nitrite as a vascular endocrine nitric oxide reservoir that contributes to hypoxic signaling, cytoprotection, and vasodilation. *Am. J. Physiol. Heart. Circ. Physiol. 291*, 2026–2035.
20. Cassoly, R., and Gibson, Q. H. (1975) Conformation, co-operativity and ligand binding in human hemoglobin. *J. Mol. Biol. 91*, 301–313.
21. Datta, B., Tufnell-Barrett, T., Bleasdale, R. A., Jones, C. J., Beeton, I., Paul, V., Frenneaux, M., and James, P. (2004) Red blood cell nitric oxide as an endocrine vasoregulator: A potential role in congestive heart failure. *Circulation 109*, 1339–1342.
22. Shaklai, N., Yguerabide, J., and Ranney, H. M. (1977) Interaction of hemoglobin with red blood cell membranes as shown by a fluorescent chromophore. *Biochemistry 16*, 5585–5592.
23. Salhany, J. M., and Shaklai, N. (1979) Functional properties of human hemoglobin bound to the erythrocyte membrane. *Biochemistry 18*, 893–899.
24. Salhany, J. M., Cordes, K. A., and Gaines, E. D. (1980) Light-scattering measurements of hemoglobin binding to the erythrocyte membrane. Evidence for transmembrane effects related to a disulfonic stilbene binding to band 3. *Biochemistry 19*, 1447–1454.
25. Shaklai, N., and Abrahami, H. (1980) The interaction of deoxyhemoglobin with the red blood cell membrane. *Biochem. Biophys. Res. Commun. 95*, 1105–1112.
26. Shaklai, N., and Sharma, V. S. (1980) Kinetic study of the interaction of oxy- and deoxyhemoglobin with the erythrocyte membrane. *Proc. Natl. Acad. Sci. U.S.A. 77*, 7147–7151.
27. Cassoly, R., and Salhany, J. M. (1983) Spectral and oxygen-release kinetic properties of human hemoglobin bound to the cytoplasmic fragment of band 3 protein in solution. *Biochim. Biophys. Acta 745*, 134–139.
28. Cassoly, R. (1983) Quantitative analysis of the association of human hemoglobin with the cytoplasmic fragment of band 3 protein. *J. Biol. Chem. 258*, 3859–3864.
29. Walder, J. A., Chatterjee, R., Steck, T. L., Low, P. S., Masso, G., Kaiser, E. T., Rogers, P. H., and Arnone, A. (1984) The interaction of hemoglobin with the cytoplasmic domain of band 3 of the human erythrocyte membrane. *J. Biol. Chem. 259*, 10238–10246.
30. Chetrite, G., and Cassoly, R. (1985) Affinity of hemoglobin for the cytoplasmic fragment of human erythrocyte membrane band 3. Equilibrium measurements at physiological pH using matrix-bound proteins: the effects of ionic strength, deoxygenation and of 2,3-diphosphoglycerate. *J. Mol. Biol. 185*, 639–644.
31. Salhany, J. M., Cordes, K. A., and Sloan, R. L. (1998) Characterization of the pH dependence of hemoglobin binding to band 3. Evidence for a pH-dependent conformational change within the hemoglobin-band 3 complex. *Biochim. Biophys. Acta 1371*, 107–113.
32. Demehin, A. A., Abugo, O. O., Jayakumar, R., Lakowicz, J. R., and Rifkind, J. M. (2002) Binding of hemoglobin to the red cell membranes with eosin-5-maleimide-labeled Band 3: Analysis of centrifugation and fluorescence lifetime data. *Biochemistry 41*, 8630–8637.
33. Salhany, J. M., Mathers, D. H., and Eliot, R. S. (1972) The deoxygenation kinetics of hemoglobin partially saturated with carbon monoxide. *J. Biol. Chem. 247*, 6985–6990.
34. Gibson, Q. H. (1969) Rapid Mixing: Stopped-Flow. *Methods Enzymol. 16*, 187–228.
35. Salhany, J. M., and Cassoly, R. (1989) Kinetics of p-mercuribenzoate binding to sulfhydryl groups on the isolated cytoplasmic fragment of band 3 protein. Effect of hemoglobin binding on the conformation. *J. Biol. Chem. 264*, 1399–1404.
36. Salhany, J. M., and Schopfer, L. M. (2001) Kinetic mechanism of DIDS binding to band 3 (AE1) in human erythrocyte membranes. *Blood Cells Mol. Dis. 27*, 844–849.
37. Leatherbarrow, R. J. (1987) *Enzfitter*, A non-linear regression data analysis program for the IBM PC (and true compatibles), Elsevier Science Publishers BV, Amsterdam, The Netherlands.
38. Liu, T., Dahlquist, F. W., and Griffith, O. H. (1997) Determination of pK(a) values of the histidine side chains of phosphatidylinositol-specific phospholipase C from Bacillus cereus by NMR spectroscopy and site-directed mutagenesis. *Protein Sci. 6*, 1937–1944.
39. Hartridge, H., and Roughton, F. J. W. (1923) The kinetics of haemoglobin part II. The velocity with which oxygen dissociates from its combination with haemoglobin. *Proc. Roy. Soc. A 104*, 395–415.
40. Dalziel, K., and O'Brien, J. R. P. (1961) The kinetics of deoxygenation of human haemoglobin. *Biochem. J. 78*, 236–245.
41. Salhany, J. M., Eliot, R. S., and Mizukami, H. (1970) The effects of 2,3-diphosphoglycerate on the kinetics of deoxygenation of human hemoglobin. *Biochem. Biophys. Res. Commun. 39*, 1052–1057.
42. Salhany, J. M., Castillo, C. L., McDonald, M. J., and Gibson, Q. H. (1975) Magnitude of subunit inequivalence for oxygen release from hemoglobin. Reinvestigation of the oxygen pulse experiment. *Proc. Natl.Acad. Sci. U.S.A. 72*, 3998–4002.
43. Kellet, G. L., and Gutfreund, H. (1970) Reactions of haemogobin dimers after ligand dissociation. *Nature (London) 227*, 921–926.
44. Hofmann, O., and Brittain, T. (1996) Ligand binding kinetics and dissociation of human embryonic haemoglobins. *Biochem. J. 315*, 65–70.
45. Lambeth, D. O., and Palmer, G. (1973) The kinetics and mechanism of electron transfer proteins and other compounds of biological interest by dithionite. *J. Biol. Chem. 248*, 6095–6103.
46. Creutz, C., and Sutin, N. (1974) Kinetics of the reactions of sodium dithionite with dioxygen and hydrogen peroxide. *Inorg. Chem. 13*, 2041–2043.
47. Kudrik, E. V., Makarov, S. V., Zahl, A., and van Eldik, R. (2005) Kinetics and mechanism of iron phthalocyanine catalyzed reduction

of nitrite by dithionite and sulfoxylate in aqueous solution. *Inorg. Chem. 44*, 6470–6475.
48. Makarov, S. V., Kudrik, E. V., van Eldik, R., and Naidenko, E. V. (2002) Reactions of methyl viologen and nitrite with thiourea dioxide. New opportunities for an old reductant. *J. Chem. Soc., Dalton Trans. 22*, 4074–4076.
49. Huang, K. T., Keszler, A., Patel, N., Patel, R. P., Gladwin, M. T., Kim-Shapiro, D. B., and Hogg, N. (2005) The reaction between nitrite and deoxyhemoglobin. Reassessment of reaction kinetics and stoichiometry. *J. Biol. Chem. 280*, 31126–31131.
50. Chu, A. H., and Ackers, G. K. (1981) Mutual effects of protons, NaCl, and oxygen on the dimer-tetramer assembly of human hemoglobin. The dimer Bohr effect. *J. Biol. Chem. 256*, 1199–1205.
51. Doyle, M. P., Pickering, R. A., DeWeert, T. M., Hoekstra, J. W., and Pater, D. (1981) Kinetics and mechanism of the oxidation of human deoxyhemoglobin by nitrites. *J. Biol. Chem. 256*, 12393–12398.
52. Fee, J. A., and Valentine, J. S. (1977) Chemical and Physical Properties of Superoxide, in *Superoxide Dismutase* (Michelson, A. M., McCord, J. M., and Fridovich, I., Eds.) pp 19−60, Academic Press, New York.
53. Wink, D. A., Darbyshire, J. F., Nims, R. W., Saavedra, J. E., and Ford, P. C. (1993) Reactions of bioregulatory agent nitric oxide in oxygenated aqueous media: Determination of the kinetics for oxidation and nitrosation by intermediates generated in the NO/O_2 reaction. *Chem. Res. Toxicol. 6*, 23–27.
54. Lewis, R. S., Tannenbaum, S. R., and Deen, W. M. (1995) Kinetics of N-nitrosation in oxygenated nitric oxide solutions at physiological pH: Role of nitrous anhydride and effects of phosphate and chloride. *J. Am. Chem. Soc. 117*, 3933–3939.
55. Huie, R. E., and Padmaja, S. (1993) The reaction of NO with superoxide. *Free Radical Res. Commun. 18*, 195–199.
56. Keshive, M., Singh, S., Wishnok, J. S., Tannenbaum, S. R., and Deen, W. M. (1996) Kinetics of S-nitrosation of thiols in nitric oxide solutions. *Chem. Res. Toxicol. 9*, 988–993.
57. Caldin, E. F. (2001) In *Mechanisms of Fast Reactions in Solution*, p 21, IOS Press, Amsterdam.
58. Koppenol, W. H., Moreno, J. J., Pryor, W. A., Ischiropoulos, H., and Beckman, J. S. (1992) Peroxynitrite, a cloaked oxidant formed by nitric oxide and superoxide. *Chem. Res. Toxicol. 5*, 834–842.
59. Lewis, R. S. (1994) Nitric oxide Kinetics in Biological Systems, Ph.D. Thesis, pp 12−16, Deptartment of Chemical Engineering, M.I.T., Cambridge, MA.
60. Eich, R. F., Li, T., Lemon, D. D., Doherty, D. H., Curry, S. R., Aitken, J. F., Mathews, A. J., Johnson, K. A., Smith, R. D., Jr., and Olson, J. S. (1996) Mechanism of NO-induced oxidation of myoglobin and hemoglobin. *Biochemistry 35*, 6976–6983.
61. Herold, S, Exner, M., and Nauser, T. (2001) Kinetic and mechanistic study of the NO-mediated oxidation of oxymyoglobin and oxyhemoglobin. *Biochemistry 40*, 3385–3395.
62. MacQuarrie, R., and Gibson, Q. H. (1971) Functional heterogeneity of the alpha and beta chains in the oxidation-reduction reaction of human hemoglobin. *J. Biol. Chem. 246*, 517–522.
63. Salhany, J. M., and Swanson, J. C. (1978) Kinetics of passive anion transport across the human erythrocyte membrane. *Biochemistry 17*, 3354–3362.
64. Sharma, V. S., Traylor, T. G., Gardiner, R., and Mizukami, H. (1987) Reaction of nitric oxide with heme proteins and model compounds of hemoglobin. *Biochemistry 26*, 3837–3843.
65. Wanat, A., Gdula-Argasinka, J., Rutkowsha-Zbik, D., Witko, M., Stochel, G., and van Eldik, R. (2002) Nitrite binding to metmyoglobin and methemoglobin in comparison to nitric oxide binding. *J. Biol. Inorg. Chem. 7*, 165–176.
66. Sutton, H. C., Roberts, P. B., and Winterbourn, C. C. (1976) The rate of reaction of superoxide anion with oxyhemoglobin and methemoglobin. *Biochem. J. 155*, 503–510.
67. Nagel, R. L., and Gibson, Q. H. (1971) The binding of hemoglobin to haptoglobin and its relationship to subunit dissociation of hemoglobin. *J. Biol. Chem. 246*, 69–73.
68. Crawford, J. H., Isbell, T. S., Huang, Z., Shiva, S., Chacko, B. K., Schechter, A. N., Darley-Usmar, V. M., Kerby, J. D., Lang, J. D., Kraus, D., Ho, C., Galdwin, M. T., and Patel, R. P. (2006) Hypoxia, red blood cells, and nitrite regulate NO-dependent hypoxic vasodilation. *Blood 107*, 566–574.
69. Mansouri, A. (1979) Oxidation of human hemoglobin by sodium nitrite-effect of beta-93 thiol groups. *Biochem. Biophys. Res. Commun. 89*, 441–447.
70. Clementi, M. E., Orsini, F., Schinina, M. E., Noia, G., and Giardina, B. (2003) Effect of nitric oxide on the transport and release of oxygen in fetal blood. *Biochem. Biophys. Res. Commun. 302*, 515–519.
71. Nagababu, E., Ramasamy, S., and Rifkind, J. M. (2006) S-Nitorsohemoglobin: A mechanism for its formation in conjunction with nitrite reduction by deoxyhemoglobin. *Nitric Oxide 15*, 20–29.
72. Nagababu, E., Ramasamy, S., and Rifkind, J. M. (2007) Intermediates detected by visible spectroscopy during the reaction of nitrite with deoxyhemoglobin: The effect of nitrite concentration and diphosphoglycerate. *Biochemistry 46*, 11650–11659.
73. Roche, C. J., Dantsher, D., Samuri, U., and Friedman, J. M. (2006) Nitrite reductase activity of sol-gel encapsulated deoxyhemoglobin. *J. Biol. Chem. 281*, 36874–36882.
74. Chu, H. Breite, A., Ciraolo, P., Franco, R. S., and Low, P. S. (2007) Characterization of the deoxyhemoglobin binding site on human erythrocyte band 3. Implications for oxygen regulation of erythrocyte properties, *Blood* [Online early access], DOI: 10.1182/blood-2007-07-100180.

BI8000819